

# Review of the rules for the operation of trains through flood water



## Copyright

© RAIL SAFETY AND STANDARDS BOARD LTD. 2015 ALL RIGHTS RESERVED

This publication may be reproduced free of charge for research, private study or for internal circulation within an organisation. This is subject to it being reproduced and referenced accurately and not being used in a misleading context. The material must be acknowledged as the copyright of Rail Safety and Standards Board and the title of the publication specified accordingly. For any other use of the material please apply to RSSB's Head of Research and Development for permission. Any additional queries can be directed to [enquirydesk@rssb.co.uk](mailto:enquirydesk@rssb.co.uk). This publication can be accessed by authorised audiences, via the SPARK website: [www.sparkrail.org](http://www.sparkrail.org).

Written by: Prof Chris Baker, Dr Hassan Hemida, Dr John Easton, Mr Dominic Flynn, Dr Michael Jesson, Birmingham Centre for Railway Research and Education, University of Birmingham.

Published: October 2015

## Executive Summary

During periods of extreme rainfall, it is not unusual for lengths of track to be flooded to a greater or lesser extent. The Rule Book GR/RT8000/M3 section 4 sets out standard procedures for operations in such conditions. These are:

- If the water depth is above sleeper level, but below the bottom of the railhead, then trains can proceed at line speed.
- If the water depth is above the bottom of the railhead, but below the top of the railhead, trains may proceed at 5 mph.
- If the water depth is above the top of the railhead, trains may only proceed if given express permission to do so by Operations Control.

Over recent years some Train Operating Companies (TOCs) have introduced variants on the above, with some reducing speeds when the water is below the bottom of the railhead and some allowing movement when the depth of water above the top of the railhead is within certain limits. The first of these in particular can have commercial implications, with penalties being incurred for running slower than the Rule Book allows. The principal aim of this project is thus to understand the physical phenomena involved in trains running through flood water and to use this understanding to revise the Rule Book provisions appropriately.

The project had a number of elements:

- A review of existing operating practice. This revealed that in the main, TOCs operated to the Rule Book, but with a range of small variations as outlined above, sometimes with different practices within one TOC for different vehicles, and sometimes with different practices for the same vehicle in different TOCs. The reasons for this variation in practice were not clear, and there was only anecdotal evidence for damage due to trains caused by running through flood water.
- The fundamental hypothesis that was made was that variations in flood water depth were caused by aerodynamically induced pressures and friction beneath the train, and due to the impact of water on the train wheels. A simple Free Surface Model (FSM) was developed which included both these effects, based on simple hydraulic theory.
- Values of the aerodynamic pressures and friction coefficients were obtained from an extensive set of steady Computational Fluid Dynamics (CFD) calculations, and information on the forces on the water due to the wheels were obtained from physical model tests with 1/32<sup>nd</sup> scale model trains running through a tray of water. These experiments also gave an indication of the amount of wheel spray that was generated. Complex unsteady CFD calculations were also carried out to verify the predictions of the FSM.
- The FSM was then used to predict the water surface displacements beneath different types of train, for different water levels and different speeds, in order to investigate the adequacy or otherwise of the Rule Book provisions.

The results of the FSM showed that the aerodynamic effects on water surface height are always small and can be neglected in all circumstances, and the variations of water depth beneath the train are caused by wheel flange contact with the water.

The immediate implication of this is that:

- When there is no flange contact with the water then there is no reason not to run at line speed.
- When the water is in contact with the flange or body of the wheel, then the water surface displacement increases along the train, and as train speed and water depths increase the displacements become larger as would be expected.
- When the water is above the bottom of the rail head, with train speeds of 5 mph as suggested by the Rule Book, water surface displacements of only a few millimetres occur along the length of a 200m train.

Thus in general, and within the limitations of the assumptions made in the calculations, the investigation confirms the adequacy of the current optimal speeds set out in the Rule Book provisions.

The results also confirm anecdotal and video evidence of the large water displacements and levels of spray that can occur when the train is moving at line speed and the wheels are in contact with the water. This suggests that some sort of early warning mechanism may be useful to alert drivers of the first train to pass through a flooded area to reduce the train speed, and this should be investigated in the future.

Finally, it should be noted that there are a number of effects that have not been taken into account in the analysis presented here. Firstly, the combined wear of wheel and rail may allow the wheel to come into contact with the water at lower depths than would otherwise be the case. Secondly, the displacement of the track due to the weight of the passing vehicle may have a similar effect. This is small for well-maintained track, of the order of a few millimetres, but can be significantly higher for poorly maintained tracks, tracks in flood prone regions, and the effect of high standing flood water on such displacements is simply not known.

## Table of Contents

Executive Summary .....	3
Table of Contents .....	5
Introduction.....	8
Current practice.....	9
Modelling methodology .....	10
Development of the free surface model .....	12
Use of the free surface model .....	14
Discussion .....	15
Conclusions.....	16
Recommendations for further work.....	16
Acknowledgements .....	17
References .....	17
Appendix 1 Current operating practice .....	19
A.    Introduction .....	20
B.    Summary of Existing National Rules .....	21
B1. Reporting flooding .....	21
B2. Running through flood water.....	21
C.    Operator practices .....	22
C.1 Virgin Trains.....	22
C.3 CrossCountry .....	24
C.4 Arriva Trains Wales.....	25
C.5 First Great Western.....	26
C.5 East Coast Trains .....	27
C.6 East Midlands Trains .....	28
D. Comparison of operator practices.....	29
E.    Implications of operating in floodwater .....	32
E.1 Additional delay minutes during flooding incidents due to operator policy .	32
E.2 Incidents of damage related to running through floodwater.....	32
E.3 Inspections following incidents of running through floodwater .....	33

F.	Conclusions .....	35
G.	References .....	36
H.	Additional Flooding Incidents .....	36
	Appendix 2 The Free Surface Model (FSM) .....	38
	Appendix 3a Steady CFD calculations .....	43
	B1. Numerical schemes.....	44
	B2. Meshing .....	45
	B3. Geometry .....	46
	D.1 Cases investigated.....	48
	D.2 Effect of train speed .....	49
	D.3 Effect of water height .....	50
	D.4 Effect of train length .....	52
	D.4 Freight train geometry.....	53
	Appendix 3b Unsteady CFD calculations .....	56
A.	Introduction .....	57
B.	Methodology.....	57
	B1. Numerical schemes and meshing .....	57
	B.2 Geometry .....	58
	B.3 Computational domains and boundary conditions .....	58
C.	Results.....	59
	C.1 Model-scale case .....	59
	C.2 Full-scale case .....	60
D.	Conclusions and recommendations for future work.....	61
E.	References .....	61
	Appendix 4 Physical model tests .....	62
A.	Introduction .....	63
B.	Experimental Setup.....	63
C.	Train Speed and Scaling .....	65
D.	Results and discussion .....	66
	D.1 Water Surface Deflection .....	66
	D.2 Wheel Splash .....	67
	D.2.1 Slight Flange Contact.....	67
	D.2.2 Full Flange Contact.....	69
	D.2.3 Main Wheel Contact.....	69



Appendix 5 Validation and use of the free surface model .....	74
A. Determination of parameters and solutions of the equations .....	75
B. Verification of model .....	77
C. Model results .....	80
D. References .....	81

## Introduction

Trains can be vulnerable to water damage when operating through flood conditions at high speeds and such damage can be of a mechanical or an electrical nature. The operational rules to operate trains through floodwater are currently specified in Rule Book GE/RT8000/M3 section 4 [1]. This allows normal operations until the water levels are up to the bottom of the rail head, a maximum speed of 5 mph for water up to the top of the railhead, and for levels higher than the railhead, movement has to be permitted by Operations Control (Figure 1). The effects of running through floodwater are well illustrated in a number of web links [2], [3], [4]. There is anecdotal evidence to suggest that some train operators believe that following the Rule Book does not appear to be sufficient to preclude damage to rolling stock and have therefore opted to implement more restrictive operational controls, (typically reduced speed even when the flood water is below the bottom of the railhead), in order to prevent vehicle damage. However, the operators are liable for any delays subsequently caused as they are deviating from the Rule Book. Operators nevertheless consider that they are being unfairly penalised in this matter.

It is thus clear there is some divergence of views in the industry around this issue, and there is a need for clarity on operational procedures. However, underlying this is a number of fundamental issues concerning the physical nature of the problem. These issues, primarily concerned with aerodynamics and hydrodynamics, need to be addressed so that the problem can be properly parameterised and understood, as a necessary precursor to a consideration of appropriate operational rules. Thus this project aimed to build an understanding of the issues that are involved, then to model them using a combination of analytical, numerical and physical techniques to lay a sound basis for understanding, and finally to apply this understanding to the development of a simple tool / set of rules that can be used to devise appropriate operational methodologies.

The precise objectives of the project were as follows:

- To review existing operating practices and existing knowledge of rolling stock types that are affected by floodwater.
- To develop a simple model that accurately predicts the behaviour of floodwater at varying water levels, train speeds and train formations
- To use the model to develop rules for the operation of trains through floodwater and to propose an update for the Rule Book in line with these revised rules.

The next section of this report outlines current practice and this is followed by a description of the modelling methodology that will be used. Descriptions then follow of the development and validation of the modelling approach through analysis, computational and physical modelling, the results of using the model and a discussion leading to a consideration of the adequacy of the Rule Book. Most of the detailed analysis and argument is contained in a series of appendices. Appendix 1 presents the survey of current practice. In Appendix 2 an aero- / hydro-dynamic model of the

phenomenon is developed as a basis for further considerations. This model required information on the pressure and shear stress distributions beneath the train which was obtained through steady Computational Fluid Dynamics (CFD) work described in Appendix 3a. Further, more complex, CFD calculations were carried out to verify the modelling approach. Information on the nature of the flow around the wheels that was obtained in the physical model tests described in Appendix 4. The various results are then collated in Appendix 5 and used to investigate flood water depths for different operational conditions and to make recommendations for updates for the Rule Book.

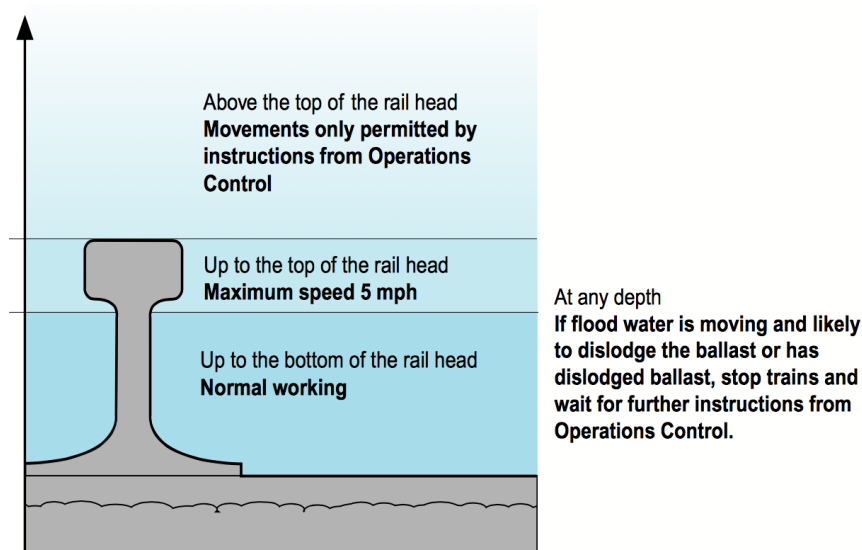


**Figure 1 Rule Book provisions for running through flood water**

## Current practice

Although the project team has only received information from a limited number of the Train Operating Companies, sufficient responses were gathered to establish that a range of different policies on the operation of vehicles through floodwaters are in use around the GB railway network (Appendix 1). In general the Rule Book requirements are followed, but with some further restrictions applied. In part, these variations seem to be linked to the physical configuration of the vehicles, with more modern classes of train that feature large amounts of undercarriage equipment being subjected to stricter speed limits, as can be seen in the case of the Class 220 / 221 and Class 390 fleets.

A summary of current practice is given in Figure 2. Here a normal operational speed of 125 mph is assumed; the various speed restriction levels have been indicated for clarity. It is notable that some variations exist between operators for vehicles of the same class – in particular the difference between policies for running the Class 221 through floodwater. It has been suggested that this stems from differing perceived risks on the part of the operators, at least in part, to do with historically high incidence rates of water ingress to bearings on Mk 3 coaches when operating through flood water at line speeds.

The damage to vehicles that have run through floodwater reported by the operators does suggest that some manner of speed restriction, as outlined by the Rule Book, is appropriate when water is above the top of the railhead. However, no reports of damage to vehicles resulting from running at the Rule Book speeds was reported to the project team, instead all instances of damage were the result of running through unreported floodwater at line speeds. The total financial costs of the damage were not obtainable by the investigators.

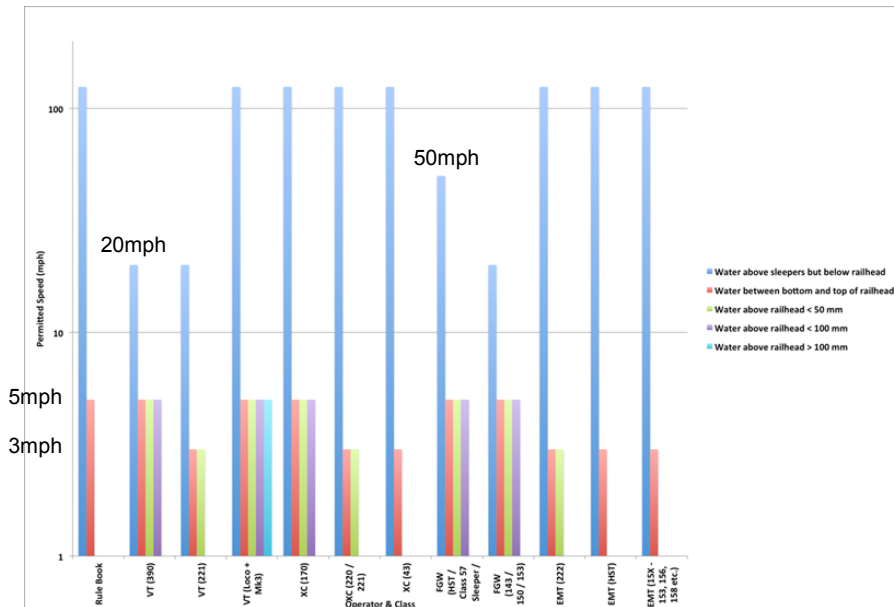


Figure 2 Current operating practice

## Modelling methodology

In the first instance, it is necessary to understand the problem under consideration so that a suitable model can be developed. The basic issue appears to be that flood water impinges on the train underside, potentially causing damage to equipment and longer term maintenance problems for bogie equipment, including axle box bearings and final drive units. There seem to be three mechanisms that could result in flood water hitting the train - vibration of the track / ballast / ground / system; the air flow and the pressure field around the train; and the rotation of the wheels when in contact with the water causing an effective friction and an upward moving spray. There is no evidence that the first issue results in water impacting upon trains, and this potential cause will not be considered further in what follows:

Now, for trains that run to the Rule Book regulations, where flood water is not above the bottom of the rail head, no part of the train should be in contact with the water. We thus hypothesise that flood water must be lifted by hydrodynamic/aerodynamic effects. The types of force that will be generated on flood water by a train are twofold:

- pressure forces that act normal to the water surface, and
- friction forces that act parallel to the surface.

The former can be expected to be significant around the train nose, where there are known to be large pressure transients [5], and to a lesser extent also around inter-carriage gaps and around the end of the train. The latter might be expected to grow in importance along the length of the train, as the underbody boundary layer develops. When trains run through water close to the rail head, the aerodynamic effects will still occur, but these will be augmented by an effective friction caused by the passage of the wheels through water and water spray lifted by the wheelsets.

As these two mechanisms are physically distinct, they need to be considered separately, and this is the fundamental basis of the work that was undertaken. The basic modelling methodology was thus as follows.

- Firstly a simple Free Surface Model (FSM) was developed of the distortion of the flood water surface under the action of transient pressure and shear (friction) forces such as those found beneath a train. The latter are caused by both aerodynamic effects and by the passage of the wheels through floodwater. This model required validation and calibration from both simple/steady and complex/unsteady Computational Fluid Dynamics (CFD) calculations and physical model tests.
- CFD calculations, in essence, solve the equations of motion for the flow of air around the train, by dividing the volume around the train into many millions of small cells, and using an iterative technique to obtain stable solutions of the equations. Typical runs may take days or weeks to carry out on multi-processor computer clusters.
- The steady CFD calculations predicted the pressure transients and shear at planes of different heights beneath a variety of train geometries and train speeds, which were then used with the FSM to investigate how the water surface height varies with train type and train speed. The calculations were verified as far as possible against existing data for the pressure transients around and beneath trains of different types.
- Physical tests of trains were carried out with trains running through floodwater at different depths and different speeds to investigate the friction and spray caused by train wheels. These consisted of 1/32<sup>nd</sup> scale model trains rolling down a slope and then through a tank of water of varying depth. This work was used to verify and calibrate the FSM and to develop a wheel friction and spray component for that model.
- A small number of more complex unsteady CFD tests were also carried out which also considered the movement of the water beneath the train. Run times were significantly increased to several weeks for the simulation of just a few seconds of real time data. These calculations were for a complete train, allowing for free surface distortion and used to verify the principles in the FSM approach, and to compare with the results of the physical modelling.
- The calibrated and verified FSM results were analysed and considerations were given to the adequacy or otherwise of the stipulations of the Rule Book.

The methodology outlined above thus combined a wide coverage of different train configurations and speeds, (using steady CFD models and physical modelling testing),

with comparisons with existing data and detailed unsteady RANS modelling for a few configurations. This is a balance between the expected low level of accuracy of the simple CFD and physical modelling methodologies, but that allows for the testing of a range of configurations with the higher expected accuracy of unsteady CFD modelling.

## Development of the free surface model

The Free Surface Model (FSM) is derived from the theory of flow in an open channel, adapted to represent the effects of a train passing over a stationary body of water [6]. The derivation of the model is given in detail in Appendix 2. It results in the following equation.

$$\frac{d\bar{h}}{d\bar{z}} = \frac{\frac{1}{2}F^2\left(\frac{dC_p}{d\bar{z}} + \frac{C_\tau}{\bar{h}}\right)\left(\frac{\rho_a}{\rho_w}\right)}{\frac{F^2}{\bar{h}} - 1 - C_p\frac{F^2}{2\bar{h}}\left(\frac{\rho_a}{\rho_w}\right)} \quad (1)$$

Here  $\bar{h}$  is the normalised water surface depth  $h/H$  where  $h$  is the actual water surface depth measured from sleeper top and  $H$  is the undisturbed water depth;  $\bar{z}$  is the normalised distance along the train  $z/H$ , where  $z$  is the distance from the train nose;  $F$  is the Froude number, the fundamental scaling parameter, given by  $F = v/(gH)^{0.5}$  where  $v$  is the train velocity;  $C_p$  is the pressure coefficient at the water surface given by  $C_p = p/0.5\rho_a v^2$  where  $p$  is the surface pressure and  $\rho_a$  is the density of air;  $\rho_w$  is the density of water; and  $C_\tau$  is the friction coefficient at the water surface, and is the sum of the friction coefficient due to the flow beneath the train and the effective friction coefficient caused by the train wheelsets passing through the flood water.

This equation is quite straightforward to solve numerically for any specified value of the pressure coefficient and friction coefficient. The water surface pressure and underbody flow friction coefficients were obtained from a wide range of steady CFD calculations that are reported in Appendix 3a, using an open source code [7], [8]. A typical plot of these results is shown in Figures 3 and 4. It can be seen that the pressure coefficient rises to a peak in front of the train, (i.e. when distances are negative), and then falls to a trough, but remains close to zero for most of the train length, although there is some variation around the train bogies and a secondary peak at the tail of the train (at about 175m). The friction coefficient is reasonably constant along the length of the train, although the presence of wheelsets etc. can be noted.

In view of the simplicity of the FSM, it does not seem appropriate to use detailed pressure and friction coefficient variations in any calculations, but rather that simplified models would be adequate. In particular we do not model the pressure and friction variations around bogies as they are judged to be of second order. We thus assume that the pressure coefficient at the front of the train is given by the simple exponential form given in Appendix 5 (equation A5.1), and specified by the peak coefficient and the distance along the train between the maximum and minimum values, whilst the friction coefficient caused by the flow beneath the train is taken as constant.

The effective friction coefficient caused by the passage of the train wheels through flood water is specified in Appendix 2 as a function of the wheel / water drag coefficient. The drag coefficient can be estimated from the results of the physical model tests using the procedure outlined in Appendix 5.

**Figure 3 Surface pressure coefficients on the ground plane positioned at the top of rail foot, bottom of the rail head, TOR and 100 mm ATOR**

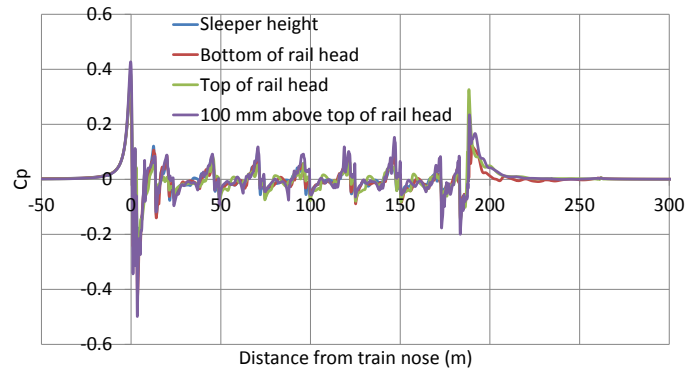
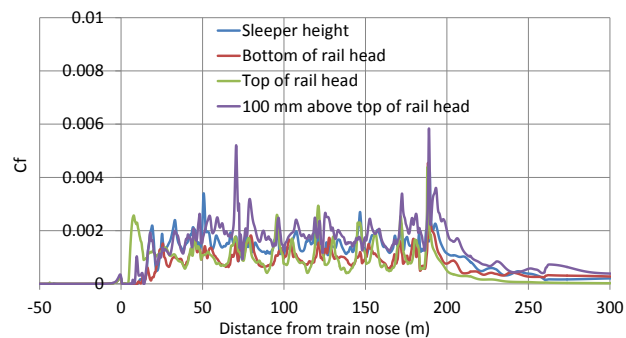


**Figure 4 Friction coefficients on the ground plane positioned at the top of rail foot, bottom of the rail head, TOR and 100 mm ATOR**



The question that immediately arises is whether or not this simple model reproduces reality in a useful way. There are a number of ways that this can be checked. The first is by a comparison of the results with visual observations / videos, a number of which can be found on the Internet, and the second is through a comparison with the physical model tests and the unsteady CFD calculations that were carried out as part of the current project. This verification is outlined in Appendix 5 from which it appears that the basic underlying surface deformation predicted by the model, (an increase in water depth around the train nose, followed by a decrease and a steady increase of the water depth along the train), is observed at full scale and in the unsteady CFD calculations.

That being said, the physical model tests and unsteady CFD calculations were significantly affected by surface tension effects that were not apparent at full scale, and it was not possible to carry out a precise quantitative comparison of this data. The other

point that is clear from the results of Appendix 5 is that the water surface deflections due to aerodynamic effects are very much smaller than those caused by the bogies.

## Use of the free surface model

The main results from the calculations of Appendix 5 are reproduced in Figures 5 to 7 below.

**Figure 5 Water surface depths – water below rail head, in contact with flange**

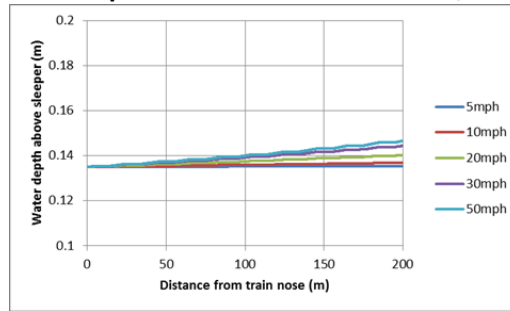


**Figure 6 Water surface depths – water at top of rail head**

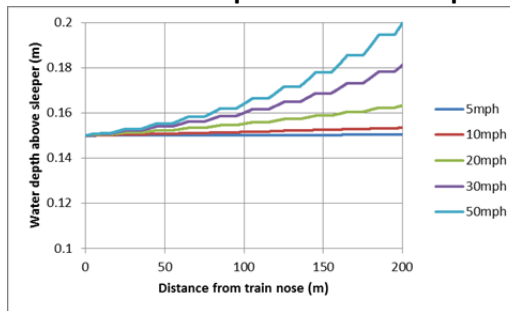
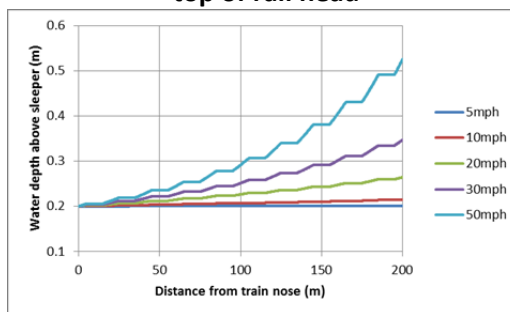


**Figure 7 Water surface depths – water below rail head, in contact with flange above top of rail head**



The results show the calculated variation in water depth for a 200m long train for three cases – when the water is below the rail head but in contact with the flange (Figure 5); when the water is at the rail head (Figure 6) and when the water is above the rail head (Figure 7). When the water is below the bottom of the railhead, there is no water surface displacement at all. The results are all similar in form, with a stepwise increase which arises from the fact that the water depth is primarily affected by the passage of the bogies. In fact it was found that the aero/hydrodynamic water depth changes were

always very small. Figure 5, where the water is below the rail head, but in contact with the flange, shows only small water depth increases along the train. Much greater depth increases are seen when the water is at the top of the railhead or above the railhead, particularly at the higher speeds (Figures 6 and 7).

## Discussion

From the results presented in the last section and in the Appendices, the following points seem to be clear.

- Aerodynamic effects on the depth of flood water beneath the train are in all cases very small and the major physical process affecting the water depth beneath the train is the effective friction imposed by the passage of the wheels and bogies through the flood water. The initial hypothesis of this work is thus shown to be incorrect. (A consequence of this is that it became unnecessary to develop a tool to devise operational methodologies). In some ways this is unfortunate, as the majority of the work that was carried out was directed towards understanding the aerodynamic effects rather than the wheel effects, which has resulted in some major assumptions being necessary in modelling the latter.
- Thus when there is no contact of the wheels with the water, there should be no increase in water depth as the train passes, regardless of the speed of the train. When there is contact between the water and wheels, then there can be expected to be an increase in water depth along and under the train. This effect increases as initial water depth increases and as train speed increases.
- For water at the top of the rail head, water depth increases along a 200m long train are confined to a few centimetres for speeds of up to 30 mph. For water above the top of rail, increases in water depths become significant at speeds of around 20 mph.
- The physical model tests suggest that for wheel contact with water below the top of the rail head, lateral and vertical spray effects will become significant at speeds of around 30 mph, and for water depths above the rail head, spray effects become of significance at around 20 mph.
- All the above points should be relatively insensitive to train type, as the primary driver of water depth changes is the small area of the wheel in contact with the water, where the geometry for different trains does not differ significantly.
- There are two potential effects that have not been considered in this work. The first is the possible deflection of the track under the weight of the passing train, causing wheel flange / water contact where it might not otherwise occur. Estimates of such values would be useful in deciding the conditions where wheel / water contact is possible. The work of [9] suggests that for well-maintained track the deflections are of the order of 2mm, but there is no information on the deflections of flooded track, or tracks in flood prone regions. The second issue is the effect of flange wear. It seems from [10] that flange depths of between 30mm and 36mm are allowable – this variation could again affect the condition for the initiation of wheel / water contact.

## Conclusions

From the points noted above the following conclusions can be drawn with regard to current operating practice.

- The original hypothesis that aerodynamic effects caused changes in flood water depths has been shown to be incorrect, and changes in water depth and spray are caused by wheel / water contact alone.
- Where there is no wheel / water contact, this research has found no evidence to support a reduction of train speeds below normal operating speeds.
- For water depths between the bottom and the top of the railhead, the results suggest that the Rule Book limit of 5 mph is appropriate.
- For water depths above the level of the rail, there are various reasons why train movements should be stopped, that are not directly concerned with the issues investigated here (ballast washing away etc) and the current Rule Book provisions are thus appropriate.

## Recommendations for further work

The work reported here suggests a number of areas where further work would be useful. These are as follows.

- The calculations presented in this report suggest that there might be scope for some relaxation of the Rule Book provisions for when the water is between the bottom and the top of the railhead, with speeds of up to 20mph being acceptable. Similarly when there is a shallow depth of water above the top of the rail, increases in water depth and spray effects can conservatively be expected to be small for speeds of up to 10 mph. However in this respect the calculations are very dependent upon aspects of the physical model tests that require validation and verification (specifically the measurement of the drag coefficient of the wheels and the nature of wheel spray). These could be best addressed by a targeted series of CFD calculations for a rotating wheel passing through water of various depths at various rotational speeds.
- The results show that predicted increases in water depths beneath the train become more significant as train speed increases. This suggests that there should be greater protection afforded to the first trains that encounter unexpected floodwater. Studies should be undertaken to identify locations where flood water depths become greater than the level of the bottom of the railhead. Although this is a problem affecting rolling stock, a more logical approach would be for real-time monitoring of water depths at trackside, initially concentrating on known problem locations. Until some advance warning of excessive flood water depths becomes available there will always be a risk of damage to the first trains entering unexpectedly deep floodwater. In principle a more sophisticated advance warning system would be possible that linked the Network Rail meteorological stations with weather radar and very short term rainfall forecasts to provide warning of possible flooding, but this would require significant development.

- It would be useful to develop procedures for operators to more fully monitor vehicles encountering flood water and consequent water-related damage, so the link and thus costs could be established on a more scientific basis than at present.
- Finally, it is clear that there is little information available on the deflection of track and sleepers due to the weight of the train with standing floodwater, and that this may affect the water depth at which water comes into contact with the flanges. Similarly the deflection of tracks in flood prone regions may be higher than normal. A short series of observations using the methodology outlined in [9] would address this issue. Similarly a survey of how much wheel / rail wear occurs in practice would allow the lowest possible position of the flange bottom relative to the bottom of the railhead to be determined and would help determine the critical point at which flanges could make contact with floodwater.

## Acknowledgements

This work was funded through RSSB Project T1052. The contributions of the project Steering Committee throughout the course of the project are gratefully acknowledged. In addition, a number of TOC and FOC representatives made invaluable contributions to the survey of existing practice for trains running through floodwater.

## References

1. RSSB (2013) "Flood water train operating rules (S165)", GR/RT8000/M3
2. YouTube (2015a) <https://www.youtube.com/watch?v=oddL3Jpn6UI>
3. YouTube (2015b) <https://www.youtube.com/watch?v=iQRT2jZxeOg>
4. YouTube (2015c) <https://www.youtube.com/watch?v=UUJ43L35E7c>
5. Quinn A. Q., Hayward M., Baker C. J., Schmid F., Priest J., Powrie W. (2010) "A full-scale experimental and modelling study of ballast flight under high speed trains", *Journal of Rail and Rapid Transit* 224, 61- 74
6. Henderson F. M. (1966) *Open Channel Flow*, Macmillan Publishing Company
7. OPEN FOUNDATION (2012) *OpenFOAM 2.1.0 User Guide* [Online]
8. Flynn, D., Hemida, H., Soper, D., Baker, C. (2014) "Detached-eddy simulation of the slipstream of an operational freight train", *Journal of Wind Engineering and Industrial Aerodynamics*, 132, 1-12
9. Le Pen L., Watson G., Powrie W., Yeo G., Weston P., Roberts C. (2014) "The behaviour of railway level crossings: Insights through field monitoring", *Transportation Geotechnics* 1 201–213

10. RGS (2010) "Railway wheelsets", Railway Group Standard GM/RT2466 Issue Three.



## Appendix 1 Current operating practice

## A. Introduction

The risk of damage and disruption as a result of flooded track is a problem for railways the world over. A 2013 RSSB report [A1.1] into the rules for operations through flood water quotes sources stating that an estimated 493,000 minutes of delay in the UK alone were attributed to flooding in the period 2004 – 2010. Damage from flooding can impact on many different elements of the railway system, including the fixed infrastructure, lineside equipment and rolling stock, and in the most extreme cases (such as flooding at Hinksey South near Oxford on the 27th November 2012) can result in thousands of minutes of delays being accrued.

Although section 4 of the Rule Book [A1.2] specifies the allowable speeds for running trains through flooded areas of the network, train operators have reported damage to vehicles occurring while working according to these procedures. Examples include water ingress into bearings and damage to under-train equipment including inverters. As a result, many train operators have adopted their own, lower speed limits for some or all of their fleets, which increases the time it takes for trains to traverse the submerged sections of track and, therefore, the number of delay minutes incurred as a result of the flooding incident.

The RSSB T1052 project aims to deliver ‘a common set of rules for the operation of trains through floodwater that does not damage rolling stock’. In practice, this means arriving at an acceptable balance between minimising the delay to services by running at speed and minimising the risk of damage to vehicles. In order to inform the modelling activities of this project, Work Package 1 reviewed existing operator practices for operating through floodwater and the findings are reported in this Appendix.

## B. Summary of Existing National Rules

The existing national procedures for the operation of trains through floodwater are outlined in section 4 of the Rule Book [A1.2]. The main actors involved include the driver, signaller and operations control (the Network Rail Route Control Manager). The procedures are split into two sections, those that govern the reporting of flooding and those for running through floodwater.

### B1. Reporting flooding

Drivers must report any floodwater with the potential to affect the passage of trains to the signaller, who in turn must report it to operations control immediately. The following information should be included as relevant:

- Has ballast been dislodged by the floodwater?
- Is the floodwater moving? If so, is it likely to dislodge ballast?
- If the floodwater is not moving, at what depth is it relative to the railhead? Is it:
  - Below the bottom of the railhead;
  - Below the top of the railhead;
  - Above the level of the railhead.

Where vehicles have been stabled in or passed through floodwater that is above the level of the bottom of the axle box, the driver must arrange for operations control to be notified.

### B2. Running through flood water

Trains may be allowed to move through floodwater if the floodwater is not moving and the ballast is unlikely to be dislodged or if the ballast has not been dislodged.

Permitted movement speeds are based on the depth of the floodwater relative to the railhead:

- If floodwater is below the bottom of the railhead, trains are permitted to continue normally;
- If floodwater is no deeper than the top of the railhead, then trains may be allowed to proceed at a maximum speed of 5 mph.

Train movements through floodwater that is above the top of the railhead are not permitted except under instruction from Operations Control.

The permitted movements through floodwater are summarised in Figure A1.1 taken from the Rule Book [A1.2].

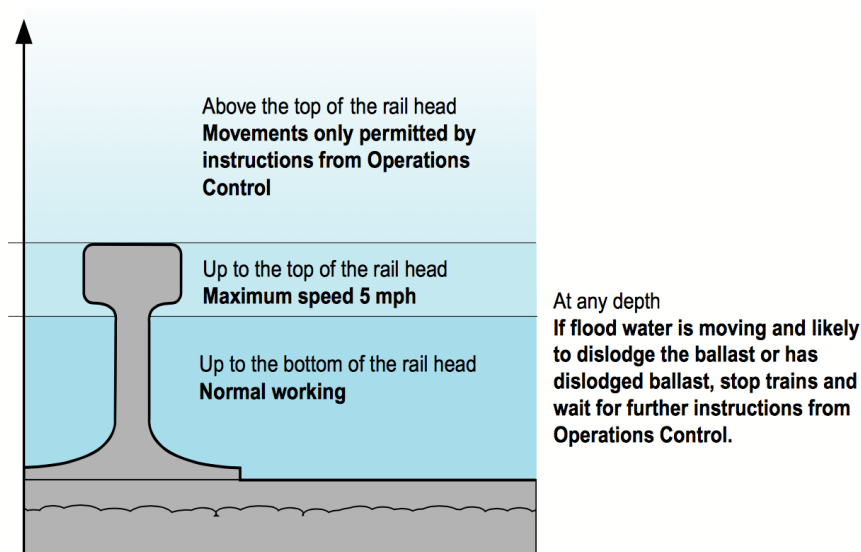


**Figure A1.1 Summary of national instructions for train movements through floodwater as outlined in the Rule Book.**

## C. Operator practices

Many Train Operating Companies adopt variations on the procedures for operating in floodwater outlined in the Rule Book, often citing damage caused to specific classes of vehicles while operating to the Rule Book as the main reason for the changes.

The operator specific instructions for vehicle movements through floodwater presented in this document are for Virgin Trains, CrossCountry, Arriva Trains Wales, First Great Western, East Coast Trains, and East Midlands Trains. Other operators may have specific policies in place (for example 750 V DC operators are unlikely to be operating any trains during flood events, but the project team had received no details of these at the time of writing this summary).

### C.1 Virgin Trains

This section is based on material from [A1.3].

Virgin Trains has a comparatively complex set of instructions for drivers that describe the permitted movements through floodwater; these have variations in both speed and depth relative to the national instructions laid out in the Rule Book.

In general (assuming floodwater is not moving sufficiently to have dislodged / risk dislodging ballast):

- If there is no water present above the top of the sleepers, services should proceed at the permitted line speed;

- If water is above the sleepers but below the railhead, services should proceed at a maximum of 20 mph;
- If water is between the bottom and top of the railhead, services should proceed at a maximum of 5 mph;
- If water is above the top of the railhead contact operations control and await instructions, if allowed to proceed speeds should not exceed those stated for floodwater levels at railhead – 5 mph (Class 390, Loco with Mk 3) or 3 mph (Class 221).

The following additional restrictions apply to specific vehicle classes / configurations of train:

- Locomotives with Mk 3 coaches:
  - If floodwater is below railhead, services should proceed as per normal working;
  - If floodwater is level with or above the railhead, the general instructions above apply.
- Class 221 (Super Voyager):
  - If floodwater is below railhead, the general instructions above apply (NOTE: this differs from CrossCountry's instructions for Class 221);
  - If floodwater is between bottom and top of the railhead, services should proceed at a maximum of 3 mph using the 'car wash' button;
  - If floodwater is above railhead by less than 50 mm, services may proceed at a maximum of 3 mph if permission is given by Operations Control;
  - If floodwater is more than 50 mm above railhead, services may not proceed.
- Class 390 (Pendolino):
  - As per the general instructions above, except that operation is only permitted when floodwater is less than 100 mm above the railhead.

Once a train has run through floodwater, Virgin requires the driver to contact the Maintenance Controller and report the depth of the floodwater, the speed at which the vehicle was travelling, and the distance it ran through the water.

Virgin Trains' instructions for movements through floodwater are summarised in Figure A1.2 taken from Virgin Trains' Modular Working Instructions [A1.3].

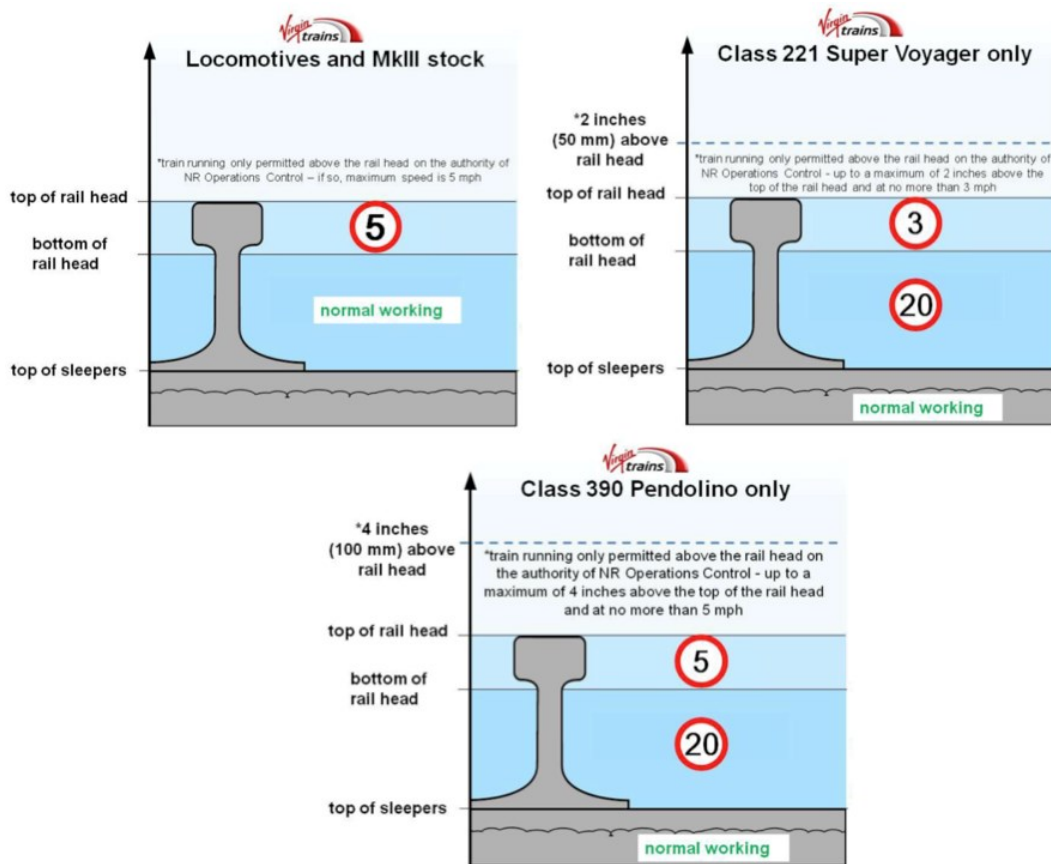


Figure A1.2 Summary of Virgin Trains instructions for train movements through floodwater.

### C.3 CrossCountry

This section is based on material from [A1.4].

For floodwater up to the bottom of the railhead, all CrossCountry services are permitted to operate at line speed, above that depth the following class-specific restrictions apply:

- Class 170 (Turbostar):
  - If floodwater is between bottom and top of the railhead, services should proceed at a maximum of 5 mph;
  - If floodwater is above railhead by less than 50 mm, services may proceed at a maximum of 5 mph if permission is given by operations control;
  - If floodwater is more than 50 mm but less than 100 mm above railhead, services may proceed at a maximum of 5 mph if permission is given by operations control.
- Class 220 / 221 (Voyager / Super Voyager):
  - If floodwater is between bottom and top of the railhead, services should proceed at a maximum of 3 mph using the 'car wash' button;

- If floodwater is above railhead by less than 50 mm, services may proceed at a maximum of 3 mph using the 'car wash' button if permission is given by operations control;
- If floodwater is more than 50 mm above railhead, services may not proceed.
- Class 43 (HST):
  - If floodwater is between bottom and top of the railhead, services should proceed at a maximum of 3 mph using the 'slow speed' button;
  - If floodwater is above the railhead, services may not proceed.

No CrossCountry service may proceed through floodwater if the depth is greater than 100 mm above the height of the railhead.

Once a train has run through floodwater, CrossCountry requires the driver to contact the Maintenance Controller and report the depth of the floodwater, the speed at which the vehicle was travelling, and the distance it ran through the water.

CrossCountry's instructions for movements through floodwater are summarised in Figure A1.3 taken from their Flood Water Operation notice [A1.4].

	Class 170	Class 220/221	HST
Any depth greater than 100mm above the top of the railhead	 Do Not Proceed	 Do Not Proceed	 Do Not Proceed
Up to 100mm above the top of the rail head	 Maximum Speed 5MPH	 Do Not Proceed	 Do Not Proceed
Up to 50mm above the top of the rail head	 Maximum Speed 5MPH	 Car Wash button	 Do Not Proceed
Up to the top of the rail head	 Maximum Speed 5MPH	 Car Wash button	 Slow Speed button
Up to the bottom of the rail head	Line Speed, in compliance with the rule book	Line Speed, in compliance with the rule book	Line Speed, in compliance with the rule book
	No Restrictions. Line Speed.	No Restrictions. Line Speed.	No Restrictions. Line Speed.

**Figure A1.3 Summary of CrossCountry instructions for train movements through floodwater.**

## C.4 Arriva Trains Wales

This section is based on material from [A1.5].

Arriva Trains Wales, who operate a mix of Class 67, 142, 143, 150, 153, 158 and 175 vehicles, has adopted a policy that allows running in floodwater with a depth of up to 100mm above the railhead. The maximum permitted speed while running through the flooded area is 5 mph. The number of any unit passing through floodwater in this way must be reported to the maintenance controller for entry into FLIRT, enabling checks to be carried out when the vehicles next return to a maintenance depot.

## C.5 First Great Western

This section is based on material from [A1.6].

For floodwaters below the level of the sleepers, or level with and above the level of the railhead, First Great Western operates its services in line with the requirements in the Rule Book. The slight exception to this is that assuming permission to move has been granted by the local signaller, a speed limit of 5 mph is explicitly stated for floodwaters above the level of the railhead, whereas the Rule Book only implies it. For floodwaters above the level of the railhead, the signaller will be advised on whether to allow the movement of services by the Engineering and Duty Control Managers.

First Great Western applies variations to the Rule Book policy on a Class-by-Class basis for floodwater above the level of the sleeper, but below the railhead. These are shown in Note 1, part of Figure A1.4, and in summary amount to a 50 mph restriction for vehicle types other than Pacer, Sprinter, and Super Sprinter DMUs, which are subject to a 20 mph restriction.

As with other operators, First Great Western does not generally permit movements of vehicles through floodwaters of depths greater than 100mm above the level of the railhead. There are, however exceptions to this rule, and factors to be considered include:

- The risks posed to customers on other trains in the area;
- Whether the vehicles involved have been fitted with enhanced seals or are already due an imminent exam;
- The potential for damage to underframe equipment, and local capabilities for checks and monitoring to take place (e.g. lineside bearing monitoring equipment, capabilities of local depots to perform equipment checks);
- The impact not running through water would have on the ability to provide train services.

In these cases, the Network Rail Route Control Manager and the 2nd Line Operations On Call Manager must be consulted, in addition to the Duty Control Manager and Engineering On Call Manager.

Height of Water	FGW Instruction	Rule Book Instruction
All Train movements are restricted to 5 mph  Water level is above this height	Do not proceed without authority from the signaller	If flood water is moving or might have dislodged ballast (irrespective of height of water), or Above the top of rail head, Movement only permitted by instruction from Operations Control
Water level is above the bottom of the rail but not the rail head	Max speed 5mph	Up to top of the rail Maximum speed 5mph
Up to the bottom of the rail head	See Note 1	Up to top of the bottom of the rail Normal working
Below the height of the sleepers	Normal Working	

Note 1:

HST	Class 57 Sleeper coaches	143	150	153	158	165/166	180
50mph	50mph	20mph	20mph	20mph	50mph	50mph	50mph

Figure A1.4 Summary of FGW instructions for train movements through floodwater.

## C.5 East Coast Trains

This section is based on material from [A1.7].

East Coast Trains' instructions on the management of vehicles running in floodwaters are the only set seen by the project team that explicitly state they are in place in order "to mitigate against the risk of water ingress into axle bearings", although First Great Western's mention problems caused to rolling stock.

East Coast allows its vehicles to operate in line with the policy outlined in the Rule Book with the exception that it, in common with Arriva Trains Wales, allows running in water above the level of the railhead, up to a maximum depth of 100mm, at 5 mph. Beyond this level, instructions from the signaller are required before movements are allowed.

## C.6 East Midlands Trains

This section is based on material from [A1.8].

East Midlands Trains has adopted a policy for the operation of services through floodwater that is basically in line with the instructions in the Rule Book. Services are allowed to proceed at line speed if the water is below the level of the railhead, and at 3 mph for floodwater that is level with the railhead (this relates to the setting of the slow speed button). Movements through water above the level of the railhead are not permitted except for the Class 222 Meridian fleet, which is allowed to proceed at 3 mph through floodwater up to 50mm above the railhead. A Network Rail Mobile Operations Manager is required to inspect the line for dislodged ballast etc. before movements through the flooded area are permitted.

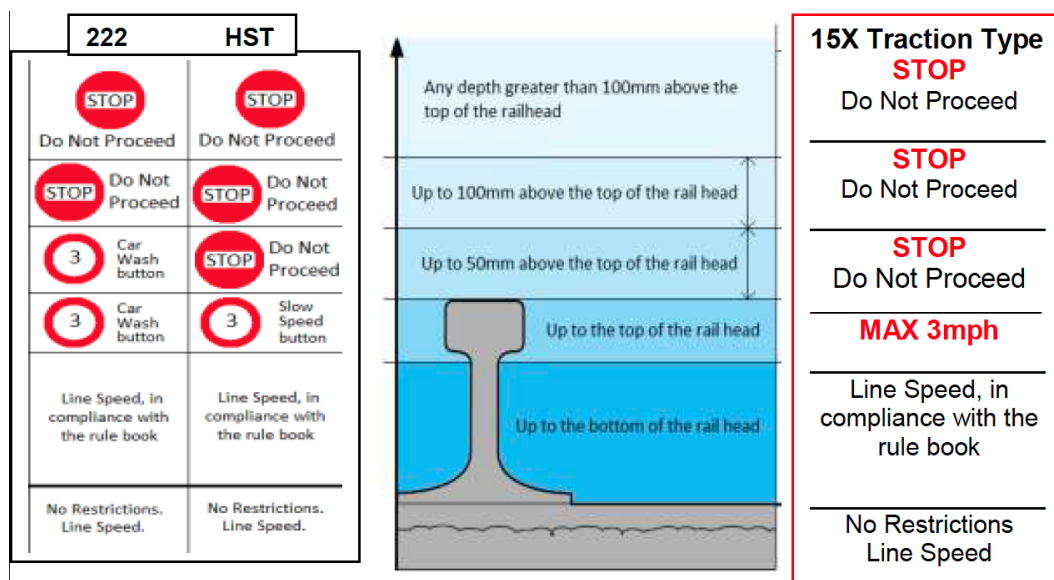


Figure A1.5 Summary of East Midlands Trains' instructions for train movements through floodwater.

## D. Comparison of operator practices

Figure A1.6 shows a comparison between the speeds permitted when moving through floodwater for a number of vehicle classes operated by Virgin Trains, CrossCountry and First Great Western. It also shows the requirements as stated in the Rule Book, which are broadly in line with those used by Arriva Trains Wales and East Coast Trains. Where the operator policy simply states that line speed is allowable, the speed has been taken to be 125 mph and a log scale has been used to prevent this from dominating the graph.

The first point to note, is that the Rule Book does not explicitly state what speeds may be permissible where floodwaters are above the top of the railhead, simply that the driver must contact operations control and await further instructions; it can safely be assumed however that the permitted movement speed, should movements be allowed, would not exceed the permitted speed for floodwater at the level of the railhead placing the speed at or below 5 mph.

Both Virgin and CrossCountry limit their Class 220 / 221 fleets to a maximum of 3 mph when running through floodwaters at railhead height, and do not permit them to run through waters more than 50 mm above the top of the railhead. This is in contrast to most other classes of vehicle, which are generally permitted to run through this depth of water at 5 mph and to continue to run in waters of up to 100 mm above the railhead given the appropriate permissions from operations control. Possible causes of this, suggested by TOC staff include: the “slow speed” carriage wash operation is set at 3mph and this is therefore more convenient to use and the location of the traction motors on the Class 220 / 221 fleets, which are mounted in the undercarriage of the vehicles, and different interpretations of the levels of business risk associated with operating at speed in floodwater.

An interesting difference between the operators can be seen in the permitted speed allowed for newer fleets when floodwater levels are below the height of the railhead. In these circumstances CrossCountry allows services to proceed at line speed, while Virgin Trains imposes a speed limit of 20 mph on their services. This is also lower than the Rule Book speed. While a direct comparison can only be drawn in the case of the Class 221 fleet (CrossCountry does not operate the Class 390) it seems strange that this should be the case.

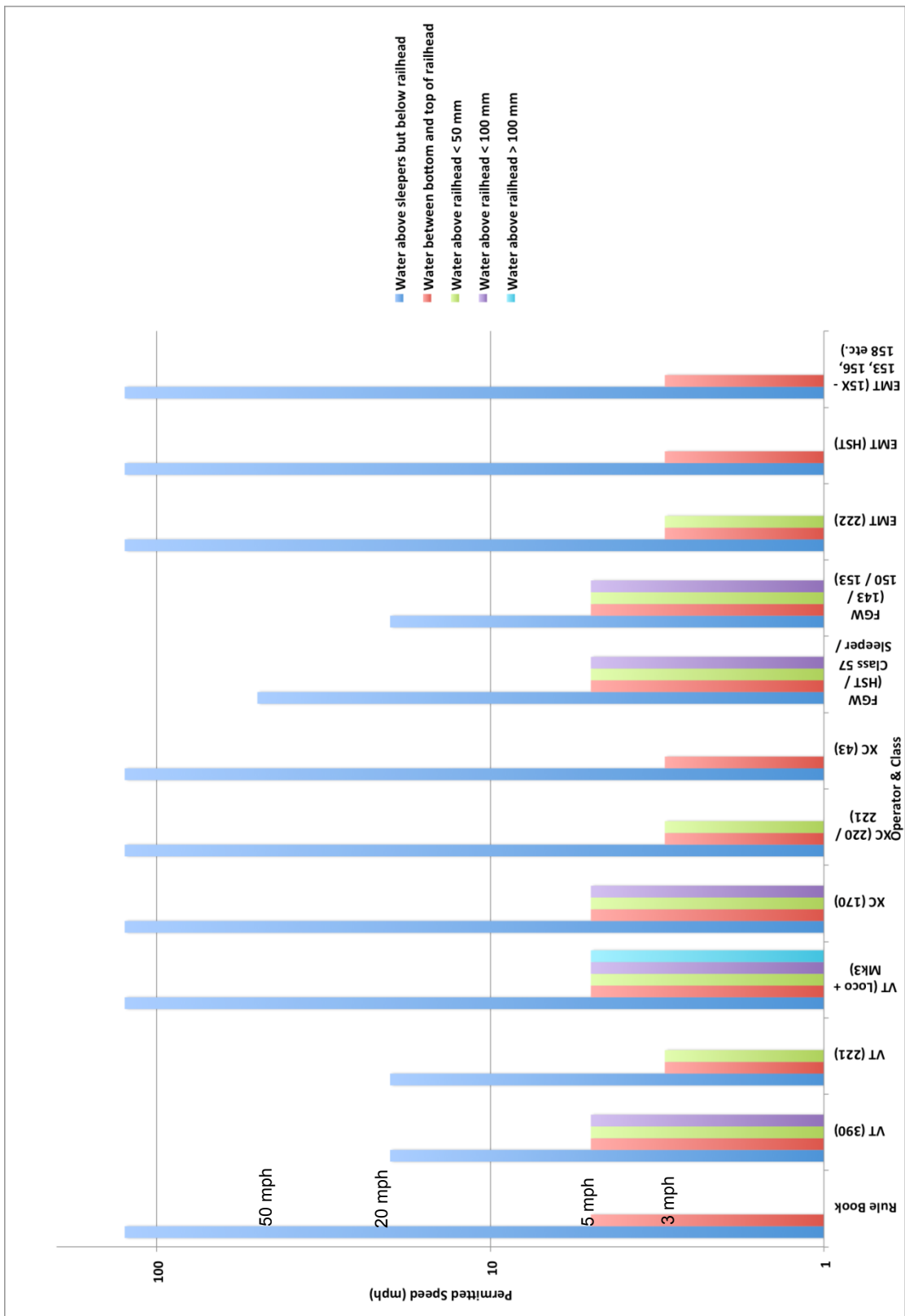


Figure A1.6 Comparison of permitted speeds under a range of floodwater levels for a range of operators

The treatment of hauled coaches also differs between the two operators. In the case of CrossCountry this refers to HST services, whereas in the case of Virgin Trains it refers to locomotives with Mk 3 stock. In either case, while both operators allow these services to run at line speed for floodwater below the railhead, when the floodwater depth exceeds this level CrossCountry limits its services to 3 mph for railhead depth and do not allow services to proceed for flooding above the railhead. Virgin Trains by comparison allows its services to continue at 5 mph for water level with the railhead (as per the national limit). The Virgin Trains Loco hauled Mk 3s are also the only fleet the project team has seen information on for which the operating policy does not place additional restrictions on services (assuming operations control clearance) if floodwaters are over 100 mm above the railhead.

Where specific operators have adopted variations to the permitted speeds outlined in the Rule Book, a number of factors have been suggested as contributing to the decision, although the precise reasoning is in many cases seemingly unknown (at least to the TOC staff interviewed).

The high rate of damage to axle bearings due to water ingress was the most commonly cited factor by TOC staff, and this was thought to have been a particular issue for HSTs / Mark 3 coaching stock early in the post-privatisation railway. Since then, improvements to the axle box sealing arrangements on these coaches are thought to have reduced this risk.

The tendency for modern vehicle designs to include large amounts of underframe equipment was also thought to be a strong contributing factor, with the risk of damage to key components, such as traction motors and inverters, being a strong disincentive to continuing to run at speed when water levels reach the railhead. Examples of this type of damage are presented in the following sections.

A further suggestion is that over time, while running through floodwater, a bow wave may begin to form at the leading edge of the bogie, effectively raising the water level at that point and therefore increasing the risk of damage to equipment, particularly that in the underframe. Videos presented to the project team have shown this effect, however as yet no specific instances of damage attributed to it have been reported to the team.

## E. Implications of operating in floodwater

In order to approximate the extent of the financial trade-off between the cost of delays resultant from operator restrictions over and above those outlined in the Rule Book and the potential costs associated with damage to rolling stock as a result of running through floodwater, the project team interviewed staff from Virgin Trains and CrossCountry about real incidents of flooding on the network and any damage that resulted.

### E.1 Additional delay minutes during flooding incidents due to operator policy

Virgin Trains staff provided the project team with access to a spreadsheet showing the delays to Virgin services attributed to flooding over the period April 2009 to November 2014. Network Rail attributed delays (DA codes X2, JK, XM) were separated from those assigned to Virgin Trains as a result of its fleet floodwater instructions (DA codes VW, MZ, MU). The restrictive policies Virgin Trains have in place are reportedly due to high incidences of damage (specifically water ingress to bearings) at the start of their franchise, before improved seals were brought in. Overall, 502 delay incidents were attributed to Network Rail during the period, with a further 18 attributed to Virgin Trains. Some incidents were common to both lists due to divided responsibility for a given delay. A large proportion of the Virgin Trains delay minutes (926 minutes) were as the result of two incidents in the winter of 2012/13, one at Kildgrove and the second just north of Kilsby tunnel. In both cases the floodwater was above the level of the sleepers but below the railhead, resulting in Virgin Trains' restriction from line speed (as per the Rule Book) to 20 mph for Class 390 and Class 221 trains being in effect.

Over the period as a whole, 47,734 minutes of delay were found to have been attributed to Network Rail as a result of flooding. In the same time frame an additional 2,115 minutes were attributed to Virgin Trains as a result of its running instructions. This amounts to approximately 4.4% of extra delay over and above the Network Rail figure.

### E.2 Incidents of damage related to running through floodwater

Although Virgin Trains staff could not provide any specific examples of damage to vehicles related to running through floodwater at speed, interviews with staff from CrossCountry proved more profitable in this area. In general, CrossCountry vehicles that run through floodwater are inspected as soon as is practical for damage, allowing the costs of repair to be correctly apportioned to Network Rail or the vehicle maintainer as appropriate. Common forms of damage resulting from running through floodwater include water ingress to bearings (particularly on older vehicles), damage to motors, and

flooding of undertrain equipment such as inverters. Bearings are particularly troublesome as they can fail quickly after an incident, and as such are re-greased or changed as a matter of course.

One incident highlighted by the CrossCountry staff interviewed, took place late in 2008 near Cullompton, Devon. It involved a Class 220 trainset on-route to Paignton, which ran through an unreported section of flooded line at approximately 100 mph. The depth of water reported after the event was around 1 inch above the railhead. The service was able to continue its journey, however it was later forced to terminate at Exeter after losing an hour.

The unit was stopped for repairs for 6 days, and damage included smashed traction case covers, due to the force of the water, and water ingress to the on-board hot axle box detection equipment and to the inverter. One estimate of the cost of repairs to the unit found by CrossCountry staff was around £12k, although there was doubt as to whether this was the total figure. In addition, an HST trainset also ran through the same floodwaters at speed, although details of the damage were not available at the time of interview.

In a separate incident in February 2011, unit 221 120 encountered floodwater near Curriehill in Scotland. Damage included water ingress to the traction electronics causing short circuits on the busbars and putting the unit out of action.

### E.3 Inspections following incidents of running through floodwater

The East Coast Trains instructions on the management of vehicles that have run through floodwater [A1.7] outline the checks to be performed on various classes of vehicles and coaching stock. This are summarised in Table A1.1.

**Table A1.1 East Coast Trains' inspections / checks following running in flood water.**

<b>Class 91</b>	<b>HST Power Car</b>	<b>HST Mk 3 Trailer Cars</b>	<b>Mk 4 Coaching Stock / DVTs</b>
Axle bearing exam	Post hot axlebox 3-point check	Axle bearing temperature stickers – check	Axle bearing examination
Gearbox external visual exam	Traction motor gearbox oil level check	Post hot axlebox 3-point check	Speed control check / adjustment
Gearbox lubricating oil sample & level check	Fuel lift pump examination; brush length check	KNORR BREMSE wheel slip / slide control unit – keypad self-test	TPWS - test
APC - test	Electronic speedometer - test		WSP probe mounting & hoses examination
Speedometer - test	TPWS - test		
TPWS - test	KNORR BREMSE wheel slip / slide control unit – keypad self-test		
WSP blow down valve – test	Traction motor interior examination		
Sanding system operation - test			

The responsible fleet engineer in conjunction with the Head of Engineering reviews the results of the checks, before being passed to the Engineering Director to be raised at the Executive Safety Group meeting.

## F. Conclusions

Although the project team has only received information from a limited number of the Train Operating Companies (Arriva, Virgin, East Coast, East Midlands, First Great Western, CrossCountry), sufficient responses were gathered to establish that a range of different policies on the operation of vehicles through floodwaters are in use around the GB railway network. In part these variations seem to be linked to the physical configuration of the vehicles, with more modern classes of train that feature large amounts of undercarriage equipment being subjected to more strict speed limits, as can be seen in the case of the Class 220 / 221 and Class 390 fleets.

Significant operating variations exist between operators for vehicles of the same class, and these are harder to explain. In particular Virgin Trains limit of 20 mph imposed on Class 221 when floodwaters are below the level of the railhead, as opposed to CrossCountry's policy of running at line speed for waters of that depth for the same class of vehicle. Industry stakeholders have suggested that this stems from differing perceived risks on the part of the operators, and Virgin Trains staff have also mentioned that their policy is, at least in part, to do with historical high incidence rates of water ingress to bearings on Mk 3 coaches.

The damage to vehicles that have run through floodwater reported by the operators does suggest that some manner of speed restriction, as outlined by the Rule Book, is appropriate when water is deeper than the railhead. However, no reports of damage to vehicles resulting from running at the Rule Book speeds was reported to the project team, instead all instances of damage were the result of running through unreported floodwater at line speeds. Some industry stakeholders have reported the formation of bow-wave effects when running through water below the level of the railhead at line speed, however no evidence of widespread damage to vehicles in current configurations due to this effect has been reported by the team, and therefore any significant impact remains to be proven by the simulations and modelling exercises in later work packages. The total financial costs of the damage were not easily obtainable, but the periods of time that units were out of service and awaiting repairs must suggest that the delay minutes accrued as a result of running below line speed are worthwhile. There is little evidence to suggest however, that running more stringent limitations than outlined in the Rule Book adds sufficient benefit to offset the added cost of delay minutes in the long term.

## G. References

- A1.1 RSSB (2013) "Flood water train operating rules (S165)". September 2013.
- A1.2 RSSB (2012) "GE/RT8000/M3 Rule Book Module M3". Issue 1, March 2012.
- A1.3 Virgin Trains (2013) "VT-IC-WI Module 2. Modular Working Instructions: Module 2 – Working of Trains". Issue 3, December 2013.
- A1.4 J Wardale (2012) "CrossCountry Operations Notice – Flood Water Operations". September 2012.
- A1.5 M Brennan. "Arriva Trains Wales Staff Brief: Flood Water".
- A1.6 First Great Western (2015) "Appendix to the Rule Book Module 9 Driving Through Flood Water". Issue 8, February 2015.
- A1.7 K Mack (2011) "East Coast - SMS10.7 Management of vehicles after running through flood water". December 2011.
- A1.8 P O'Brien (2012) "New notice case – East Midlands Trains: Flood Water Operation". December 2012.

## H. Additional Flooding Incidents

Further reported incidents of flooding on the rail network can be found in the following Network Rail Incident Log summaries. A selection is listed below.

### **Log for 15th – 21st August 2008**

20th August, flooding at Livingston North, risk of voiding required track to be tamped.

### **Log for 4th – 10th December 2009**

6th December, flooding at Clay Cross tunnel, indirectly resulted in wrong way routing.

### **Log for 17th – 23rd September 2010**

23rd September, flooding at Shap, broken bodyside window and bogie damage due to ballast thrown up on impact with floodwater.

### **Log for 1st – 7th October 2010**

3rd October, flooding at Winterbutlee tunnel, 309 minutes delay.

### **Log for 2nd – 8th September 2011**

6th September, flooding at Woodacre, 3018 minutes delay.

### **Log for 23rd – 29th November 2012**

25th November, flooding at Athelney CCTV crossing at 12 inches above rail height, 5217 minutes delay.

25th November, flooding between Darlington South and East Cowton leading to track circuit failures, 3985 minutes delay.

26th November, bridge ECM1/342 closed due to severe flooding, 4437 minutes delay.

27th November, flooding at Stretton following earlier incident of train striking high ballast, 1765 minutes delay.

27th November, flooding at Hinksey leading to damaged track circuits, 20445 minutes delay.

28th November, flooding at Preston le Skerne, 1836 minutes delay.

**Log for 31st January – 6th February 2014**

4th – 5th February 2014, Dawlish, washed out sea wall, 468 delay minutes and line blocked until 4th April.

**Log for 12th – 18th September 2014**

18th September, Box tunnel, vehicle trapped in floodwater with passengers on board, 97 minutes delay.

## Appendix 2 The Free Surface Model (FSM)

## A. Introduction

This Appendix outlines the development of the Free Surface Model that was developed as the primary tool to investigate the variation of water depth beneath trains. Extensive physical model tests and CFD calculations were carried out to verify and calibrate aspects of this model and these are described in Appendices 3 and 4. In Section B of this Appendix the outline of the model and the basic equations are set out. The effect of wheels is presented in Section C, and the overall form of the model discussed in Section D.

## B. Basic equations

We begin with the shallow water St. Venant equations for unsteady open channel flow [A2.1]. These are given by:

$$h \frac{\partial u}{\partial x} + u \frac{\partial h}{\partial x} + \frac{\partial h}{\partial t} = 0 \quad (\text{A2.1})$$

$$\frac{\partial u}{\partial t} + u \frac{\partial u}{\partial x} + g \frac{\partial h}{\partial x} - g(S_0 - S_f) = 0 \quad (\text{A2.2})$$

Here  $h$  is the water depth,  $x$  is the distance along the channel and  $u$  is the mean channel velocity at  $x$ .  $S_0$  is the channel gradient and  $S_f$  is the friction slope, effectively the friction at the channel bed expressed in terms of an equivalent (negative) channel slope. Equations (A2.1) and (A2.2) are derived from a straightforward application of the continuity and energy equations to the gradually varied unsteady flow along an open channel.

To apply this to our situation of a train passing above a stationary mass of water, we firstly adopt a co-ordinate system moving with the train – effectively letting the train be stationary and the water move beneath it at the speed of the train – and solve the above equations for the parameter  $z = vt - x$ , where  $v$  is the train speed.  $z$  is thus the distance measured from the nose of the train. This results in the equations

$$-h \frac{\partial u}{\partial z} - u \frac{\partial h}{\partial z} + v \frac{\partial h}{\partial z} = 0 \quad (\text{A2.3})$$

$$v \frac{\partial u}{\partial z} - u \frac{\partial u}{\partial z} - g \frac{\partial h}{\partial z} - g(S_0 - S_f) = 0 \quad (\text{A2.4})$$

If we assume  $v \gg u$ , then after some manipulation this results in the equation

$$\frac{dh}{dz} = \frac{S_0 - S_f}{\frac{v^2}{gh} - 1} \quad (\text{A2.5})$$

This is very similar to the equation for steady, gradually varied open channel flow. We express it in a non-dimensional form by letting:

$$F = \frac{v}{(gH)^{0.5}} \quad (\text{A2.6})$$

$$\bar{z} = \frac{z}{H} \quad (\text{A2.7})$$

$$\bar{h} = \frac{h}{H} \quad (\text{A2.8})$$

where  $H$  is the undisturbed flow depth, and  $F$  is a Froude number, which gives

$$\frac{d\bar{h}}{d\bar{z}} = \frac{S_0 - S_f}{\frac{F^2}{\bar{h}} - 1} \quad (\text{A2.9})$$

We model the deformation of the water surface due to the train by assuming that the slope term  $S_0$  can be modified to allow for pressure and friction variations along the train (which are a function of  $z$ ) and assume that the friction term  $S_f$ , which represents the friction on the bottom of the water mass, is zero.

An equivalent value of the slope can be calculated by assuming that the gravitational force pulling water down the channel due to a slope can be equated to the force due to the pressure difference and the friction along the channel.

$$\rho_w g \delta x h S_0 = h \frac{dp}{dz} \delta z + p \frac{dh}{dz} \delta z + \tau \delta z \quad (\text{A2.10})$$

Here  $p$  is the pressure at the water surface due to the passage of the train,  $\frac{dp}{dz} \delta z$  is the pressure difference along a length  $\delta z$ ,  $\tau$  is the surface shear stress and  $\rho_w$  is the water density. This gives

$$S_0 = \frac{1}{2} F^2 \left( \frac{dC_p}{d\bar{z}} + \frac{C_p}{\bar{h}} \frac{d\bar{h}}{d\bar{z}} + \frac{C_\tau}{\bar{h}} \right) \left( \frac{\rho_a}{\rho_w} \right) \quad (\text{A2.11})$$

where  $C_p$  is the pressure coefficient given by

$$C_p = \frac{p}{0.5 \rho_a v^2} \quad (\text{A2.12})$$

$\rho_a$  is the density of air and  $v$  is the train speed.  $C_\tau$  is the surface shear stress coefficient that represents the shear stress caused by the passing train and is given by

$$C_\tau = \frac{\tau}{0.5 \rho_a v^2} \quad (\text{A2.13})$$

It will be seen below that there is a further component of shear stress due to the wheels passing through the flood water. The above equations result in the following general equation.

$$\frac{d\bar{h}}{d\bar{x}} = \frac{\frac{1}{2} F^2 \left( \frac{dC_p}{d\bar{z}} + \frac{C_\tau}{\bar{h}} \right) \left( \frac{\rho_a}{\rho_w} \right)}{\frac{F^2}{\bar{h}} - 1 - C_p \frac{F^2}{2\bar{h}} \left( \frac{\rho_a}{\rho_w} \right)} \quad (\text{A2.14})$$

This equation is easily solvable numerically, and enables the variation in water surface depth to be calculated for applied values of the pressure coefficient and shear stress coefficient. The pressure coefficient variation will be largest around the train nose, but will also vary to a limited extent along the length of the train, particularly around inter-car gaps. One would expect the shear stress coefficient to be broadly constant along the train, but it could be increased significantly around bogies due to the effects of wheel sets.

## C. Wheel and spray component

The effect of the train wheels in producing friction beneath the train has already been taken into account through the train friction coefficient. There are however two other effects of the train wheel sets that occur when the wheels are running through water and these will be considered in this section. The first of these is the extra effective friction caused by the passage of the wheels through the water. This gives an increment to the shear stress coefficient  $C'_\tau$  given by

$$C'_\tau = \left(\frac{\rho_w}{\rho_a}\right) C_D A_w / A_b \quad (\text{A2.15})$$

Here  $C_D$  is defined as

$$C_D = \frac{D}{0.5\rho_w A_w v^2} \quad (\text{A2.16})$$

$D$  is the overall drag of the bogie  $A_w$  is the frontal area of the submerged part of the wheels, and  $A_b$  is the plan area of a bogie. To calculate  $A_w$  we assume that the flange width and depth is 0.03m, the wheel width is 0.1m and  $w$  is the depth of the submerged portion of the wheel. This results in the following approximate expressions.

$$A_w = 2(0.03w) \quad (\text{A2.17})$$

when  $w < 0.03\text{m}$  (ie when the water surface is below the rail head) and

$$A_w = 2(0.03^2 + 0.1(w - 0.03)) \quad (\text{A2.18})$$

when  $w > 0.03\text{m}$  (ie when the water surface is above the rail head and only in contact with the wheel flanges). The factor of two allows for the area of the two front wheels of the bogie.  $A_b$  is given by the bogie length (5m) multiplied by the track width (1.5m).

The second effect of the wheels is to cause spray that impinges on the underside of the train. The data that is available for spray from the physical model tests (see Appendix 4) is significantly affected by scale effects, and can only offer broad guidance. However it will be seen that there are reasonably well defined critical velocities for which spray occurs, with a larger velocity for flange only / water contact than for full wheel / water contact, and the approach taken in the use of the model will be to indicate where spray effects are likely to be significant, rather than specifying them in a quantitative manner (Appendix 5).

## D. Discussion

If we put together the equations representing the aerodynamic effects on the water surface and the effects of the wheels we obtain the following composite equation.

$$\frac{d\bar{h}}{d\bar{x}} = \frac{\frac{1}{2}F^2 \left( \frac{dC_p}{dz} + \frac{C_\tau + \left(\frac{\rho_w}{\rho_a}\right) C_D A_w / A_b}{h} \right) \left(\frac{\rho_a}{\rho_w}\right)}{\frac{F^2}{h} - 1 - C_p \frac{F^2}{2h} \left(\frac{\rho_a}{\rho_w}\right)} = \frac{\frac{1}{2}F^2 \left( \frac{dC_p}{dz} \left(\frac{\rho_a}{\rho_w}\right) + \frac{C_\tau}{h} \left(\frac{\rho_a}{\rho_w}\right) + \frac{C_D A_w}{h A_b} \right)}{\frac{F^2}{h} - 1 - C_p \frac{F^2}{2h} \left(\frac{\rho_a}{\rho_w}\right)} \quad (\text{A2.19})$$

There are two points of significance that should be noted at this point. The first is that there is a potential instability in the solution when the denominator goes to zero. However a brief consideration of magnitudes shows that this will occur for very low vehicle speeds of the order of 2 to 5 mph, when it can be expected that surface tension effects will dominate over aerodynamic effects and wheel drag effects will also not be significant.

Secondly the aerodynamic terms contain the ratio of the densities of air and water which is of course very small. Thus if, as expected, the wheel drag coefficient is of order unity, whatever the values of the pressure and friction coefficients, then the aerodynamic terms will be small, and the water surface deflections caused by these effects will also be correspondingly small. Thus if this is the case equation (A2.19) becomes

$$\frac{d\bar{h}}{d\bar{x}} = \frac{\frac{1}{2}F^2 \left( \frac{C_D A_w}{h A_b} \right)}{\frac{F^2}{h} - 1} \quad (\text{A2.20})$$

If the Froude number is large, this results in the expression

$$\frac{d\bar{h}}{d\bar{x}} = \frac{1}{2} \left( C_D \frac{A_w}{A_b} \right) \quad (\text{A2.21})$$

In Appendix 5, calculations are presented that investigate the relative effects of the aerodynamic and wheel terms, and then this methodology is used to systematically investigate the variation of water depth beneath trains of different types.

## E. Reference

A2.1 Henderson F. M. (1966) *Open Channel Flow*, Macmillan Publishing Company



## Appendix 3a Steady CFD calculations

## A. Introduction

The steady computational fluid dynamics (CFD) simulations reported in this Appendix were used to obtain the surface pressure and friction coefficients on the ground plane beneath a variety of train types, speeds, and lengths. The height of the ground plane was varied relative to salient rail features to represent different levels of flooding.

## B. Methodology

The simulations were conducted using the Reynolds-averaged Navier-Stokes (RANS) method, which is based around the time-averaged Navier-Stokes equations. This method has the main advantage of providing data in a relatively short time in comparison to other available methods, and was the ideal choice because of the number of simulations required. Due to the formulation of the RANS equations, closure is required in the form of a turbulence model, and it is the turbulence model which is partially responsible for a solution's accuracy. The  $k-\omega$  shear stress transport model [A3a.1] was used because of its reliable performance in external vehicle aerodynamics simulations [A3a.2]

The software used to conduct the simulations was OpenFOAM 2.1.1 [A3a.3] which is an open-source CFD code and is freely available to users around the world. The advantage of open-source codes is that the requirement for licenses is bypassed because running a simulation across multiple processors with a commercial code can become extremely expensive in terms of license fees for larger simulations. Due to the number of simulations that were required within the time-frame of this project, using multiple nodes for each simulation was necessary.

Open source codes can have poor reputations on the grounds of fidelity, but the majority of solvers in OpenFOAM have been verified against the European Research Community on Turbulence, Flow and Combustion (ERCOFTAC) database as well as being validated in numerous external vehicle aerodynamics research projects [A3a.4, A3a.5] and thus the software's fidelity can be considered sound.

### B1. Numerical schemes

Discretisation is the process of reducing continuous equations, such as partial differential equations, into linear algebraic equations which allows them to be more easily solved. The accuracy of a numerical simulation is strongly dependent on the choice of discretisation scheme, and to this end it was ensured that all simulations in this work were discretised to second order accuracy in both space and time, where appropriate. In the steady simulations, the convection term was discretised using a

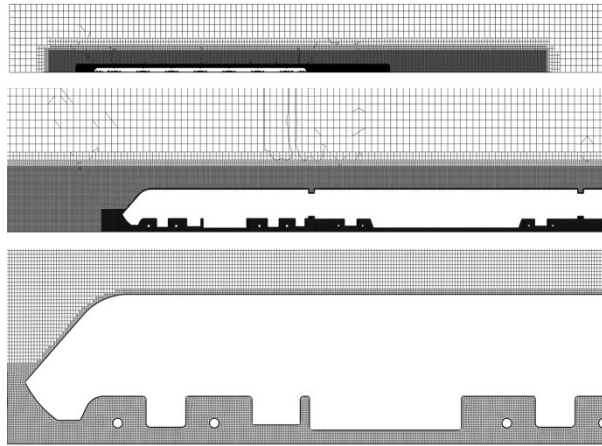
second order upwind differencing scheme and gradient terms were treated with second order central differencing.

The solver used for the simulations was simpleFoam which is a steady-state, incompressible, turbulent flow solver based around the semi-implicit method for pressure-linked equations (SIMPLE) algorithm [A3a.6] which was developed to decouple the pressure and velocity terms in the Navier-Stokes equations.

## B2. Meshing

In order to solve the governing equations across the domain, the domain must first be broken down into a series of discrete volumes. The discretised governing equations are then solved across the volume of the cells in the mesh and this is the technique known as the finite volume method. The computational meshes used in the simulations were generated using SnappyHexMesh (SHM) which is an automatic mesh generation utility in OpenFOAM. The advantage of SHM over other automatic meshing software is that it can generate meshes that are dominated by hexahedral cells which allows for fewer cells to be needed for a given case than would be required for tetrahedral cells. Hexahedral meshes are also generally more accurate than the tetrahedral meshes, but are usually more difficult to generate in complex geometry.

The resolution of a mesh defines the amount of detail which can be captured in the flow. In the steady simulations the requirement for the level of detail was lower than in the unsteady case because the flow gradients which were solved for remained stationary due to the time-averaged flow. The flow gradients near the walls i.e. the boundary layer, require very flat cells known as prism layers. For the simulations, five prism layers were used on each surface and it was ensured that the non-dimensional distance,  $y^+$ , of the first cell to the wall was between  $y^+=50$  and  $y^+=100$ , so a wall function could be applied appropriately. Wall functions ensure that the logarithmic velocity profile near the wall is enforced without the need for very fine mesh cells to directly resolve this profile. Computational costs can be significantly reduced using wall functions, although the use of an approximation method does add further uncertainty and perhaps inaccuracy into the simulations.



**A3a.1 Mesh density levels used in the steady CFD simulations**

Figure A3a.1 shows the mesh around the Class 43 power car for the steady RANS simulations. A fine mesh density box has been placed beneath the vehicle to ensure that the highly-complex flow is resolved as accurately as reasonably possible. Furthermore, the medium mesh density is shown to extend 50 m behind the train to allow for near wake resolution.

### B3. Geometry

The train geometries used in this research were the Class 43 high speed train (HST) power car, Mk 3 coaches, the Class 66 locomotive and fully-loaded FEA-B container wagons (Figure A3a.2). These were chosen in consultation with the stakeholders to represent a range of vehicle nose and underbody shapes. The setup of each consist considered is shown in Figure A3a.3.

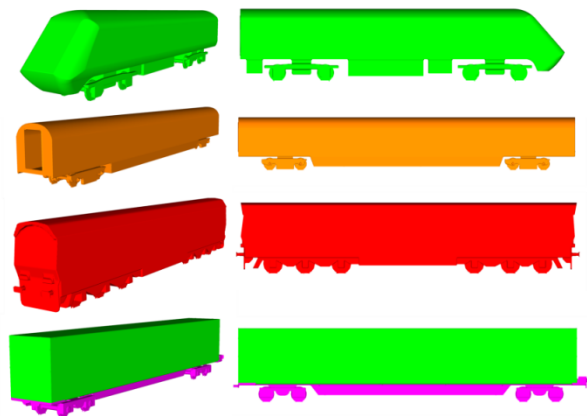


**Figure A3a.2 Class 43 locomotive, Mk 3 passenger coach, Class 66 locomotive and fully-loaded FEA-B container wagon**

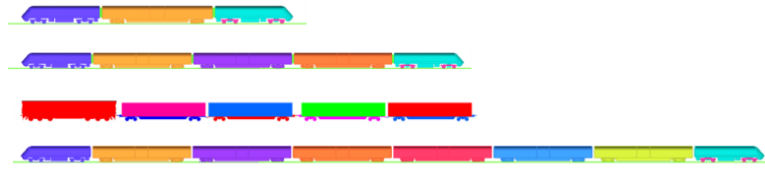


**Figure A3a.3 Train configurations used in the steady CFD simulations**

## C. Computational domain and boundary conditions

The boundary conditions used in a CFD simulation define the flow problem, and if poorly-posed they can have a detrimental effect on the accuracy and stability of a solution. For the steady RANS cases, the motion of a train passing over static ground was replicated by applying the same velocity as the inlet to the ground plane. This is known as the train-fixed frame of reference and has been used in many numerical simulations of train slipstreams in recent years [A3a.7, A3a.4]. The inlet to the domain was set as a fixed-velocity boundary condition and the outlet was set as a zero-pressure outlet.

The computational domain used in the steady simulations was sized in accordance with the CEN recommendations [A3a.8]. The calculations were carried out at full scale. The inlet is positioned 75 m ahead of the train and the outlet is at least 250 m behind the train (see Figure A3a.4). The roof and sides of the domain are set as no-slip walls, and are approximately 33 m from train side.

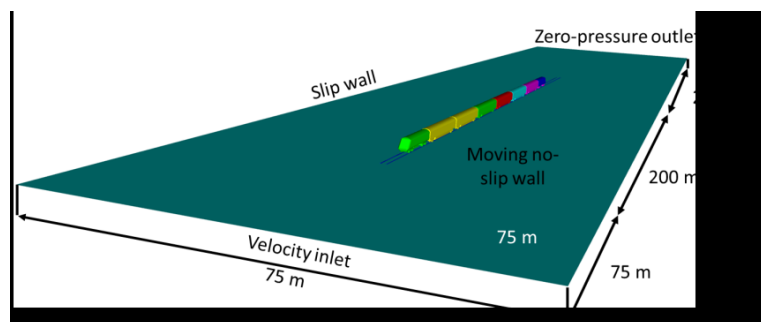


**Figure A3a.4 Computational domain and boundary conditions for the steady CFD simulations**

## D. Results

The simulations were used to obtain surface pressure and frictional forces on the ground plane to be fed into the free-surface model developed in Appendix 2.

The data presented in the following sections are normalised quantities where a dependence on speed, ground position, or train length was tested. The pressure coefficient,  $C_p$ , and friction coefficient,  $C_\tau$ , are calculated as

$$C_p = \frac{2(p-p_\infty)}{\rho_a v^2} \quad (\text{A3a.1})$$

and

$$C_\tau = \frac{2\tau}{\rho_a v^2} \quad (\text{A3a.2})$$

where  $\rho_a$  is the air density,  $p$  is the pressure,  $p_\infty$  is the freestream pressure measured upstream of the train,  $\tau_w$  is the wall shear stress and  $v$  is the train speed. The wall shear stress is obtained from the logarithmic velocity profile

$$\frac{u}{u_*} = \frac{1}{\kappa} \ln\left(\frac{uy}{v_a}\right) \quad (\text{A3a.3})$$

and

$$u_* = \sqrt{\frac{\tau}{\rho_a}} \quad (\text{A3a.4})$$

to give

$$\tau = \frac{\kappa^2 u^2}{\rho_a \ln\left(\frac{uy}{v_a}\right)^2} \quad (\text{A3a.5})$$

where  $y$  is the distance above the ground,  $v_a$  is the kinematic viscosity,  $\kappa$  is the Karman constant and  $u$  is the air velocity relative to the ground. In this work, the velocity samples were made at 0.001 m above the ground plane.

## D.1 Cases investigated

To cover the range of possible train speeds, train geometries and flood water levels, two matrices of the simulations conducted are presented in Table A3a.1 and Table A3a.2. The two tables consider the four train geometries shown in Figure A3a.3, and show which train speed and ground position they are used for.

**Table A3a.1 Train speeds investigated using each train geometry**

	30 mph	70 mph	100 mph
3 Car HST		X	
5 Car HST		X	
8 Car HST	X	X	X
Freight		X	

**Table A3a.2 Ground plane positions investigated using each train geometry**

	Bottom of rail foot $h=0m$	Bottom of rail head $h=0.1m$	Top of rail $h=0.15m$	100 mm above top of rail $h=0.25m$
3 Car HST		X		
5 Car HST		X		
8 Car HST	X	X	X	X
Freight		X		

## D.2 Effect of train speed

The pressure coefficients on the ground plane positioned at the bottom of the rail head at the centre of track are shown in Figure A3a.5 for the 30 mph, 70 mph and 100 mph cases; the train used was the eight car Class 43 train. The effect of the train speed on the pressure coefficient remains almost negligible along train length, but in the near wake a strong dependence is shown. The dependence of the tail peak on the train speed is likely to be due to the reduction in downwash effect caused by flow separation from the slanted roof of the rear power car, which one would expect to be susceptible to Reynolds number effects. The largest tail peak is from the 30 mph case, followed by the 100 mph case and then the 70 mph case.

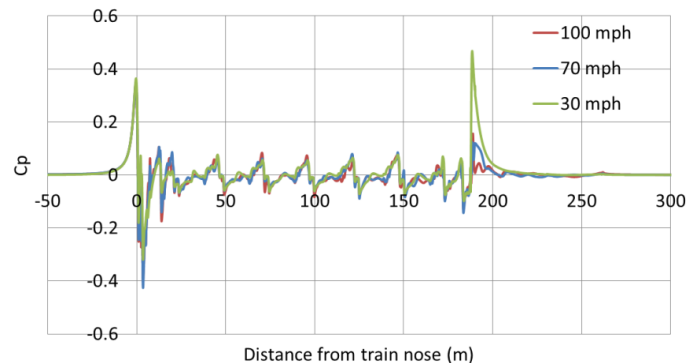


**Figure A3a.5 Pressure coefficients on ground plane at the bottom of rail head for the 30 mph, 70 mph and 100 mph cases**

Figure A3a.6 shows the friction coefficients on the middle of the ground plane which is positioned at the bottom of rail head for the 30 mph, 70 mph and 100 mph cases. The 30 mph case shows the highest friction coefficient values along the entirety of the train, with the peak value occurring in the near wake. The friction coefficients from the 70

mph and 100 mph cases remain more comparable due to the closer train speeds. Table A3a.3 summarises the data presented in Figure A3a.5 and Figure A3a.6.

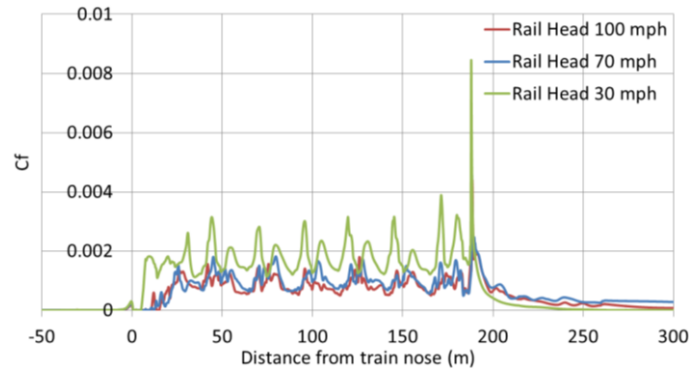


**Figure A3a.6 Friction coefficients on ground plane at the bottom of rail head for 30 mph, 70 mph and 100 mph**

**TableA3a.3 Pressure and friction characteristics on the ground at the bottom of rail head for the 30 mph, 70 mph and 100 mph cases**

	Nose peak Max $C_p$	Nose peak Min $C_p$	Nose $\Delta C_p$	Peak to peak distance $\Delta x$ (m)	Tail $C_p$	Max $C_\tau$	Mean $C_\tau$
30 mph	0.36	-0.32	0.68	4.02	0.47	0.0085	0.0018
70 mph	0.35	-0.43	0.78	4.03	0.12	0.0045	0.0010
100 mph	0.35	-0.40	0.75	4.06	0.16	0.0044	0.0009

### D.3 Effect of water height

Surface pressure and frictional forces were obtained on the ground plane at several vertical positions in order to establish the effect of water height on its deflection in the free-surface model developed in Appendix 2. The positions considered were at the top of the rail foot, bottom of the rail head, top of rail (TOR) and 100 mm above top of rail (100 mm ATOR)

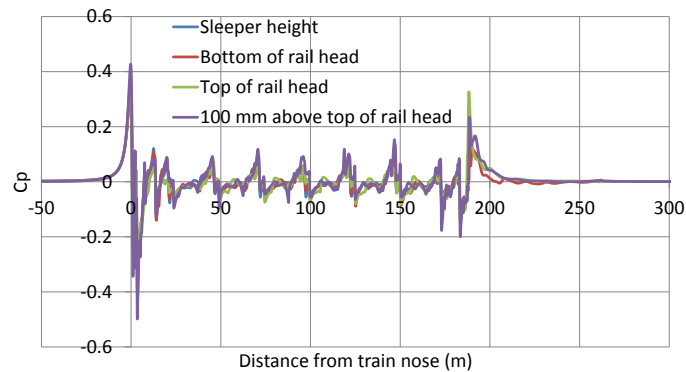


**Figure A3a.7 Surface pressure coefficients on the ground plane positioned at the top of rail foot, bottom of the rail head, TOR and 100 mm ATOR**

Figure A3a.7 shows the pressure distribution on the ground plane at four vertical positions. The positive nose pressure pulse are very similar for all ground plane positions although the 100 mm ATOR shows the greatest negative nose pressure peak. Along the train length a general similarity is seen between all water heights and in the near wake the TOR ground case has the greatest positive tail peak. Overall, it is observed that the height of the ground plane has little influence on the surface pressure.

Figure A3a.8 shows the friction coefficients on the ground plane for the same four vertical positions considered in Figure A3a.7. Along the train length there is little difference between the friction coefficient values, but the highest tail peak occurs when the ground position is placed at the foot of the rail head.

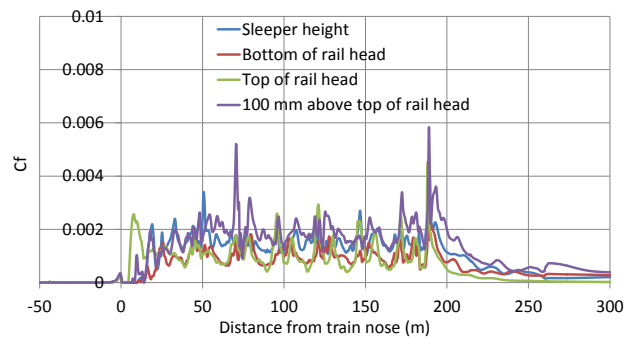


**Figure A3a.8 Friction coefficients on the ground plane positioned at the top of rail foot, bottom of the rail head, TOR and 100 mm ATOR**

Table A3a.4 summarises the data from Figure A3a.7 and Figure A3a.8.

**Table A3a.4 Pressure and friction characteristics on the ground positioned at the top of rail foot, bottom of rail head, TOR and 100 mm ATOR, for a train travelling at 70 mph**

	Nose peak Max $C_p$	Nose peak Min $C_p$	Nose $\Delta C_p$	Peak to peak distance $\Delta x$ (m)	Tail $C_p$	Max $C_\tau$	Mean $C_\tau$
Rail Foot	0.33	-0.26	0.59	4.47	0.05	0.0042	0.0015
Rail Head	0.35	-0.43	0.78	4.03	0.12	0.0045	0.0010
TOR	0.38	-0.34	0.73	3.88	0.32	0.0044	0.0011
100 ATOR	0.43	-0.50	0.93	3.68	0.23	0.0058	0.0019

## D.4 Effect of train length

The cases considered above have shown that there is relatively little difference between the pressure and frictional coefficients on the ground plane for different train speeds and vertical positions of the ground plane. However for all of the cases considered so far, the train geometry and length has been kept constant.

Figure A3a.9 shows the effect of varying train length on the surface pressure on the ground plane. In the nose region little variation is observed as would be expected because of the similar train geometry. Again, the magnitudes of the surface pressure along the train lengths are very similar. Overall it can be seen that train length has little or no noticeable effect of the surface pressure coefficients on the ground plane.

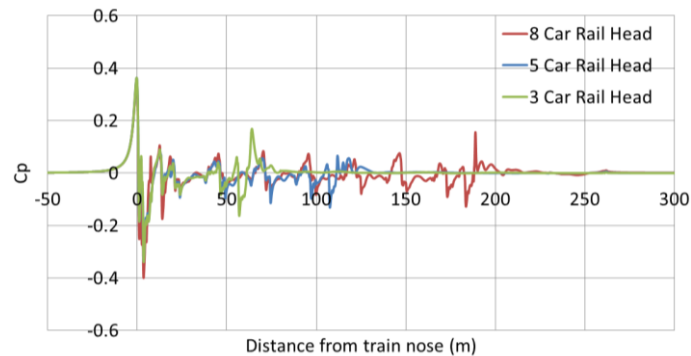


**Figure A3a.9 Surface pressure coefficients on the ground plane at the bottom of rail head for three, five, and eight car trains at 70 mph**

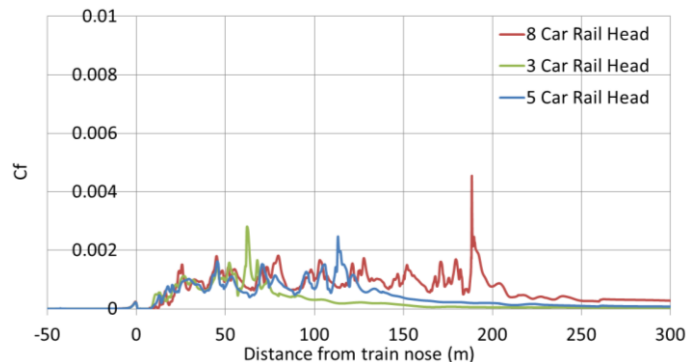


**Figure A3a.10 Friction coefficients on the ground plane at the bottom of rail head for three, five, and eight car trains at 70 mph**

Figure A3a.10 shows the friction coefficients on the ground plane beneath the three car, five car and eight car trains travelling at 70 mph. The main difference observed between the friction coefficients on the ground plane is the magnitude of the peak in the near wake. The variation of friction coefficient in the wake with train length was anticipated because it is known from the literature that trains of different lengths will have different levels of slipstream development and thus velocities around the trains will be different

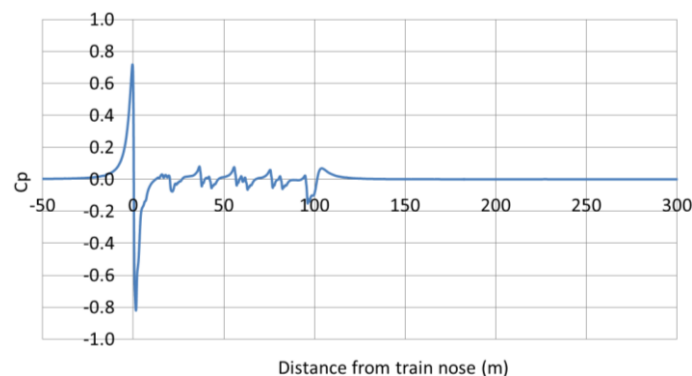
[A3a.9]. Table 5 collates salient features of the pressure and friction coefficient data on the ground plane shown in Figure A3a.9 and Figure A3a.10.

**Table A3a.5 Pressure and friction characteristics on the ground positioned bottom of rail head for train sets consisting of three, five and eight cars travelling at 70 mph**

	Nose peak Max $C_p$	Nose peak Min $C_p$	Nose $\Delta C_p$	Peak to peak distance $\Delta x$ (m)	Tail $C_p$	Max $C_r$	Mean $C_r$
3 Car	0.36	-0.34	0.70	4.02	0.17	0.0028	0.0008
5 Car	0.36	-0.34	0.70	3.99	0.28	0.0025	0.0009
8 Car	0.35	-0.43	0.78	4.03	0.12	0.0045	0.0010

#### D.4 Freight train geometry

Due to the fact that freight trains cause higher slipstream velocities and pressures at trackside than passenger trains [A3a.10], motivation was therefore provided to investigate the pressure and friction coefficients on the ground plane beneath a Class 66 hauled container freight train.



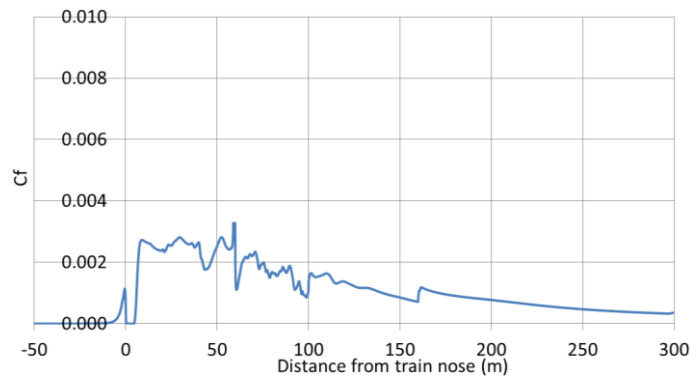
**Figure A3a.11 Pressure coefficient on the ground plane beneath a Class 66 locomotive hauling four fully-loaded FEA-B container wagons**

Figure A3a.11 shows the pressure coefficient on the ground plane beneath the freight train. It is observed that the peak-to-peak pressure coefficient values at the front of the train are approximately four times greater than those seen for the passenger train cases due to the less aerodynamically refined geometry of the train.

Figure A3a.12 shows the friction coefficient on the ground plane beneath the freight train. The friction coefficient is largely greater than is observed for the passenger train

cases due to the relatively rough underbody region and the low clearance between the air dam at the front of the locomotive and the ground.

The pressure and friction data presented in Figure A3a.11 and Figure A3a.12 are given in Table A3a.6.



**Figure A3a.12 Friction coefficient on the ground plane beneath a Class 66 locomotive hauling four fully-loaded FEA-B container wagons**

**TableA3a.6 Pressure and friction characteristics on the ground beneath the freight train**

	Nose peak Max $C_p$	Nose peak Min $C_p$	Nose $\Delta C_p$	Peak to peak distance $\Delta x$ (m)	Tail $C_p$	Max $C_\tau$	Mean $C_\tau$
Freight	0.72	-0.82	1.54	1.89	0.067	0.0033	0.0017

## E. Conclusions

Steady numerical simulations were conducted to obtain pressure and frictional force coefficients on a ground plane which would act as inputs to a free-surface model being developed in Appendix 2.

The steady RANS calculations investigated the effect of differing train speeds, train geometries and ground plane heights on the pressure and friction coefficients. The main conclusions drawn from the results are as follows.

- Pressure coefficients around the nose were independent of train speed, but some dependence on speed was noted in the near wake coefficients. As the distance from the train to the ground plane increased, the pressure coefficient peaks reduced in magnitude. The freight train peaks were higher than the passenger train peaks.

- The friction coefficient was broadly constant along the length of the train, although the positions of bogies and inter car gaps could be seen. The friction coefficients decreased somewhat with train speed, but little effect of ground plane- train spacing was seen.
- Train length only had small effects on the pressure and skin friction coefficients.

## F. References

- A3a.1 Menter, F. (1993) "Zonal two-equation k-w turbulence model for aerodynamic flows", 24th Fluid Dynamics Conference. Orlando, FL Paper 93-2906: AIAA
- A3a.2 Ortega, J., Salari, K. & Storms, B. (2008) "Investigation of tractor base bleeding for heavy vehicle aerodynamic drag reduction", *Aerodynamics of heavy vehicles II: Trucks, buses and trains*, 41, 161-78
- A3a.3 OPEN FOUNDATION (2012) OpenFOAM 2.1.0 User Guide [Online]
- A3a.4 Flynn, D., Hemida, H., Soper, D., Baker, C. (2014) "Detached-eddy simulation of the slipstream of an operational freight train" *Journal of Wind Engineering and Industrial Aerodynamics*, 132, 1-12.
- A3a.5 Hemida, H., Baker, C. J., Gao, G. (2012) "The calculation of train slipstreams using Large-Eddy Simulation", *Proceedings of the Institution of Mechanical Engineers, Part F: Journal of Rail and Rapid Transit*, 228, 25-36
- A3a.6 Patankar, S. V. & Spalding, D. B. (1972) "A calculation procedure for heat, mass and momentum transfer in three-dimensional parabolic flows", *International Journal of Heat and Mass Transfer*, 15, 1787-1806.
- A3a.7 Huang, S., Hemida, H., Yang, M. (2014) "Numerical calculation of the slipstream generated by a CRH2 high-speed train", *Proceedings of the Institution of Mechanical Engineers, Part F: Journal of Rail and Rapid Transit*, doi: 10.1177/0954409714528891
- A3a.8 CEN (2011) "Railway applications - Aerodynamics - Part 4: Requirements and test procedures for aerodynamics on open track", 2010, BS EN 14067-6:2010.
- A3a.9 Muld T. W., Efraimsson G. Henningson D. S. (2014). "Wake characteristics of high-speed trains with different lengths". *Proceedings of the Institution of Mechanical Engineers. Part F, Journal of Rail and Rapid Transit*, 228, 4, 333-342
- A3a.10 Sterling, M., Baker, C. J. (2008) "A study of the slipstreams of high-speed passenger trains and freight trains", *Proceedings of the Institution of Mechanical Engineers, Part F: Journal of Rail and Rapid Transit*, 222, 177-193.

## Appendix 3b Unsteady CFD calculations

## A. Introduction

The unsteady multiphase simulations were conducted in order to capture the interaction between the air and water beneath the train as a result of aerodynamic effects. The multiphase simulations were initially conducted at model-scale to replicate the physical model described in Appendix 4, and then at full-scale in order to provide a more direct comparison to the free-surface model.

## B. Methodology

The multiphase simulations were conducted using a volume of fluid phase-fraction interface-capturing method using the Reynolds-averaged Navier-Stokes (RANS) method, which is based around the time-averaged Navier-Stokes equations. Due to the formulation of the RANS equations, they require closure in the form of a turbulence model, and it is the turbulence model which is partially responsible for a solution's accuracy. In this project, the  $k-\omega$  shear stress transport model [A3b.1] was used because of its reliable performance in external vehicle aerodynamics simulations [A3b.2]. The phase-fraction interface-capturing method has the advantage of using a static mesh unlike other multiphase methods where the mesh moves relative to the free surface; an approach which reduces computational expense by avoiding the need for remeshing at each time step.

The software used to conduct the simulations was OpenFOAM 2.3.0 [A3b.3], which is an open-source code and therefore is freely available to users around the world, and a variant of that described in Appendix 3A.

### B1. Numerical schemes and meshing

For general details of the basic numerical scheme and the meshing characteristics, see Appendix 3. The resolution of a mesh defines the amount of detail which can be captured in the flow. In the multiphase simulations a fine mesh was required beneath the train because of the small anticipated deflection of the water's surface. The flow gradients near the walls i.e. the boundary layer, require very flat cells known as prism layers. For the steady cases, five prism layers were used on each surface and it was ensured that the non-dimensional distance,  $y^+$ , of the first cell to the wall was between  $y^+=50$  and  $y^+=100$ , so a wall function could be applied appropriately. Wall functions ensure that the logarithmic velocity profile near the wall is enforced without the need for very fine mesh cells to directly resolve this profile. Computational costs can be significantly reduced using wall functions, although the use of an approximation method does add further uncertainty into the simulations.

Figure A3b.1 shows the mesh projected onto a cut-plane at the centre of track. The high-density mesh region is seen to extend almost to the centre of the axles, and is 24 cells deep (not including prism layers on the ground plane). As mentioned above, a detailed

description of the deflection of the free-surface was required which necessitated a very fine mesh. In order to maintain stability of the solver, the mesh around the water phase was required to be the same across the entire domain, and it was this requirement which was responsible for the high computational cost of the simulations.

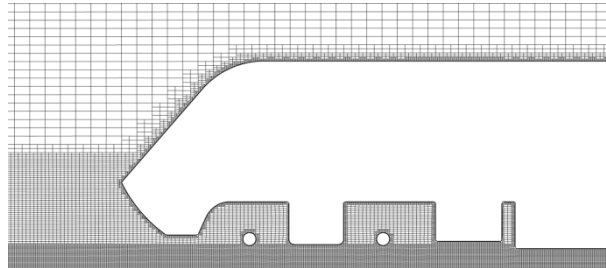


**Figure A3b.1 Mesh projected onto a cut plane at centre of track for the multiphase simulations**

## B.2 Geometry

The simulations were conducted using one Class 43 power car and one Mk 3 coach (Figure A3b.2). In order to replicate the physical experiments the simulations were initially performed at 1/32<sup>nd</sup> scale, and then at full-scale to provide direct comparison to the free-surface model. At model-scale the total train length was approximately 1.25 m whereas at full-scale the total train length was 40 m.



**Figure A3b.2 Vehicle geometry used in multiphase simulations**

## B.3 Computational domains and boundary conditions

The multiphase simulations were conducted in a somewhat small domain as a result of the requirement for the high mesh density close to the air-water interface, and the desire to avoid a prohibitively computationally expensive simulation (Figure A3b.3). The main issue with this size of domain is the resulting high blockage-ratio, which may result in some speed up around the train and higher than predicted air velocities than would otherwise have been the case, and this must be acknowledged as a limitation of the study.

The requirement for two fluid phases gave the need for two inlets; one for air and the other for water. The water inlet extended from the ground plane to the top of the rail (TOR) which was 0.0045 m at model-scale and 0.15 m at full-scale, which meant that the water level was set at the top of rail level. The velocities of the fluids at each inlet were set as 5 m/s for the 1/32<sup>nd</sup> scale case and 13.4 m/s (30 mph) for the full-scale case. The

domain roof was set as a total pressure outlet, and the outlet was given a zero-gradient condition for the water phase. In order to complete the train-fixed frame of reference, the ground plane and rails were set to have the same velocity as the air and water. The surface tension between the air and the water was 0.07 Nm.

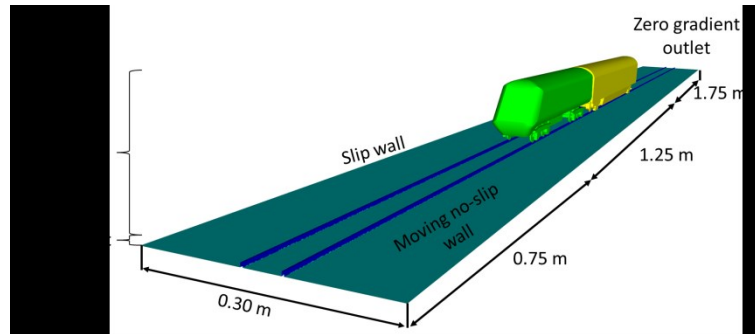


**Figure A3b.3** Computational domain used in the multiphase simulations

## C. Results

### C.1 Model-scale case

The model-scale multiphase simulations were conducted in order to replicate the physical model, and act as a means to obtain further data about the water's deflection beneath the train. Figure A3b.4 shows an isosurface of the water phase set at 0.5, which means that the surface will be generated where the air and water phases interact. At this scale little obvious deflection of the water's surface can be discerned in front of the train. Figure A3b.5 shows the calculated water surface deflections (with full scale equivalent values) at a much larger scale. The deflection of the water is observable at this scale but with peak deflections of only 7 mm.

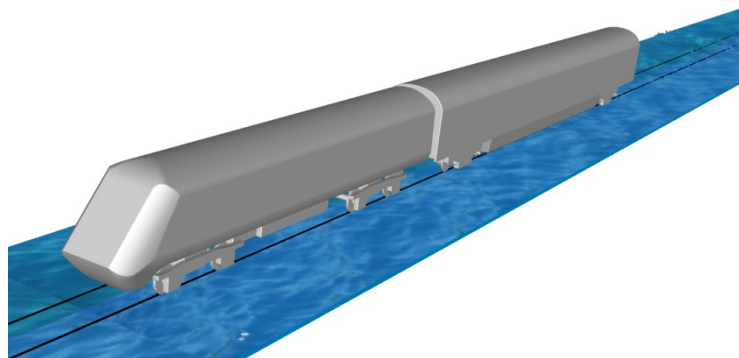


**Figure A3b.4** Visualisation of air-water interface in the computational domain

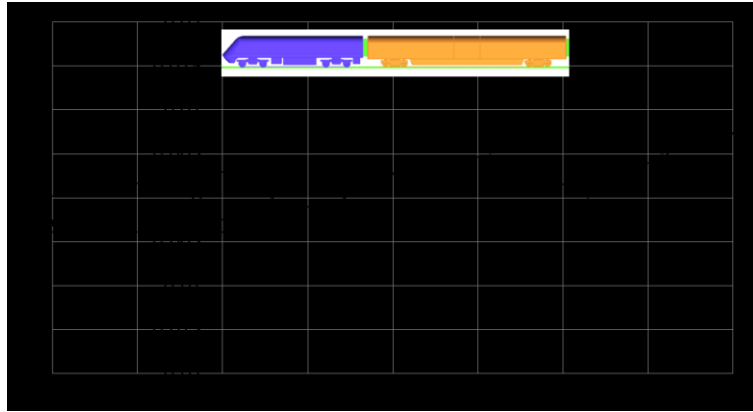


**Figure A3b.5 Time-averaged water surface deflection along train length for the model-scale simulations**

Figure A3b.6 shows the instantaneous pressure coefficient on the air-water interface. In the nose region of the train a positive-negative is observed and the nose pressure transients are broadly in agreement with anticipated values for a passenger train. Unsteadiness in the pressure signal along the length of the passenger coach increases until the near wake where the disturbance becomes significant enough to cause a numerical instability.

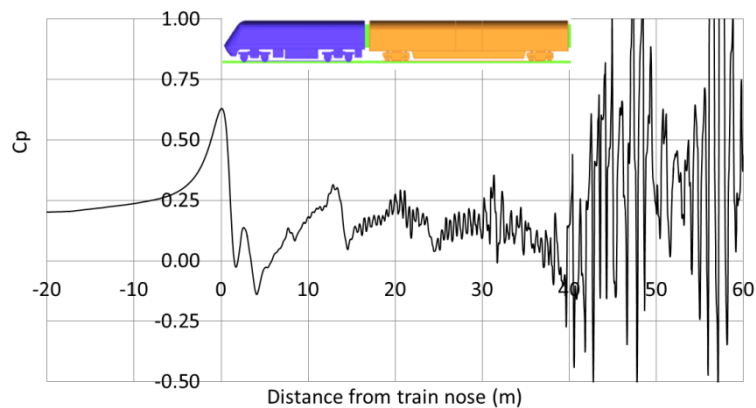


**Figure A3b.6 Instantaneous pressure coefficient on the water's surface at centre of track**

## C.2 Full-scale case

As discussed above, the lack of deflection of the water's surface due to aerodynamic effects was primarily because of the dominance of surface tension at model-scale. In order to determine whether any deflection would occur at higher speeds, another case was developed at full-scale with the train travelling at 30 mph. However, due to the relatively small computational domain used, the blockage ratio was high which has implications on the boundary conditions which in turn lead to excessive numerical instabilities and the results did not converge. The results are not shown here.

## D. Conclusions and recommendations for future work

The multiphase simulations were conducted in order to provide comparison to the physical experiments and to act as validation for the free-surface model. From the unsteady multiphase calculations the following conclusions are drawn:

- In the model-scale simulation only small deflections of the water's surface was noticed due to the dominance of surface tension.
- At full-scale the simulations were very unstable due to the high blockage ratio of the computational domain and no useful results could be obtained.

Based on the results presented, the following recommendations for future work are made:

- The multiphase simulations did not consider relative movement between the wheel and the rail and hence wheel splashing effects were omitted. A numerical model should be developed which will allow for this effect to be quantified.

## E. References

- A3b.1 Menter, F. (1993) "Zonal two-equation k-w turbulence model for aerodynamic flows", 24th Fluid Dynamics Conference. Orlando, FL Paper 93-2906: AIAA
- A3b.2 Ortega, J., Salari, K. & Storms, B. (2008) "Investigation of tractor base bleeding for heavy vehicle aerodynamic drag reduction", *Aerodynamics of heavy vehicles II: Trucks, buses and trains*, 41, 161-78
- A3b.3 OPEN FOUNDATION (2012) OpenFOAM 2.1.0 User Guide [Online]

## Appendix 4 Physical model tests

## A. Introduction

This Appendix describes model-scale physical simulations of trains running through flood water performed at the University of Birmingham. These simulations were designed to quantify water surface fluctuations caused by the pressure field around the nose and along the body of a train passing through the flood water, to investigate the wetting of train components due to splashing from the wheels, and to provide data from which the drag coefficient of wheels running through floodwater could be determined.

## B. Experimental Setup

The physical simulations were performed using a gravity-driven, 1:32 scale test rig consisting of a vertical 'U'-shaped track and two train models (Figure A4.1). The scale was chosen due to its suitability for construction of the rig in the University of Birmingham Civil Engineering labs, and it being the modelling standard 'Gauge 1' scale, allowing track and wheels to be purchased off-the-shelf.

The double track rig has 2m high arms and a horizontal base of approximately 3.5m which runs through a 4m long tank. This tank may be filled with water to simulate flooding of the track. Each arm of the rig is fitted with a mechanism to secure a train model at the highest point of the arm. Release of the train models is triggered using a control box connected to the two mechanisms, allowing the two models to be released simultaneously and hence pass in the middle of the tank.



**Figure A4.1 The T1052 Physical Simulation Rig**

The train models each consist of a single Class 43 locomotive and single Mark 3 carriage. The train bodies were custom-built for the project by Derwent Patterns Ltd., with the

underbody modelled using simple blocks with little detailing. The wheels are off-the-shelf, 32mm diameter wheels, and are attached to simple models of bogies. It should be noted that the wheel flange is not to scale as an over-sized flange is necessary to prevent the model from derailing. The wheel dimensions are given in Figure A4.2 below.

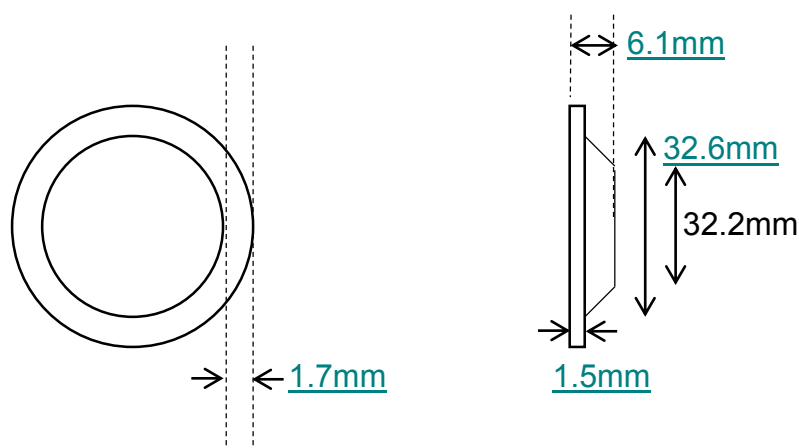


**Figure A4.2 Model wheel dimensions**

Three sets of experimental runs were made. The first were designed to measure the deflection of the water surface due to the pressure field created by a passing train. These runs were conducted using a single train. Initial runs used water levels at the top of the railhead, but the water depth was then increased to the maximum possible due to no measurable deflection being seen.

The second set of experiments, examining wheel splash onto the body of the train, used three water depths. At full-scale, water depths are usually referenced relative to the railhead, and in these terms the three depths were bottom of railhead, (level with) top of railhead and over railhead (approximately one railhead height again above the railhead). Due to the oversized flanges, however, these water depths at model scale do not give the same contact between the wheel and water as would be the case at full-scale where, for example, bottom of railhead would result in no contact with the wheel flanges. To emphasise this difference, the three depths in the simulations are referred to as slight flange contact (SFC), full flange contact (FFC) and main wheel contact (MWC) respectively.

Being a gravity-driven rig, train model speed is determined solely by the starting position (height) on the track. A single starting position, that of the release mechanism, was used for the first set of experiments and the passing train runs of the second set. Eight starting positions were used for the single train runs in the second set of experiments, giving eight speeds. The same eight starting positions were used for each water depth, and these positions were approximately evenly spaced along the length of the track arms. The speeds achieved are detailed in 'Train Speed and Scaling' below. The third set of experiments used an additional water depth (up to the underbody of the train), to

allow validation of the wheel drag component of the model. This set of experiments additionally included multiple (ten) runs from each of a number of starting positions, allowing run-to-run variation of speed to be evaluated, and a confidence interval for the mean speed to be deduced. One set of ten runs was also performed with no water contact, to further investigate the wheel drag effect.

With the small water depths used in the experiments, surface tension was expected to have an effect. Surfactants were added to the water in the tank to reduce surface tension as much as possible.

Experimental runs were recorded at 800 frames per second for slow motion playback, using a Sony NEX-FS700RH camera.

## C. Train Speed and Scaling

The speed of the train models was calculated using the videos of the experimental runs. For each run, the video was advanced until the nose of the train was at the edge of the frame and the time noted. The video was then advanced until the tail of the train reached the same position, and the time noted again. The train model speed was then calculated using the train length and the difference in the two times. Estimates of the measurement uncertainties are  $\pm 3\text{mm}$  for the train length, and  $\pm 0.04\text{s}$  for the times, (based on the resolution of the timestamp on the playback software), and the uncertainty in the model speeds is calculated as approximately  $0.007\text{ m/s}$  ( $0.1\text{ mph}$  full-speed).

The pressure-driven water surface displacement as the train passes through the flood water, is governed by the Froude number:

$$Fr = \frac{v}{\sqrt{gh}} \quad (\text{A4.1})$$

where  $v$  is the train speed,  $g$  is gravitational acceleration and  $h$  is the water depth. Full- and model-scale equivalence is achieved when the Froude number is equal for the two systems, giving a velocity scale which is the square-root of the (1:32) length scale, ie 1:5.7.

Scaling for the wheel splash experiments is a complex issue. Based on the velocity at which droplets will be projected tangentially from the outer edge of the wheel/flange, scaling will be linear (1:32). Conversely, aerodynamic resistance on the droplets (which will affect the distance travelled) is proportional to the square of the velocity, but is also proportional to their cross-sectional area. The size of the smallest droplets will be governed by surface tension, which will be the same at model and full-scale, though the use of surfactants to reduce surface tension may affect this. Pick-up of water by the surfaces of the wheel will be determined by surface roughness, which will not be equivalent at the model- and full-scales. Taking these factors into account, the wheel

splash experiments may only be used to give qualitative results – full-scale experiments are required to fully investigate these effects.

Model-scale train speeds are given in Table A4.1 for each of the eight starting positions, for each of the three water depths used in the wheel splash experiments. Equivalent full-scale speeds, based on Froude number equivalence, are also given for reference.

#### A4.1 Train model speeds and full-scale equivalent speeds

Starting Position	SFC		FFC		MWC	
	V (model, m/s)	V (full, mph)	V (model, m/s)	V (full, mph)	V (model, m/s)	V (full, mph)
1	4.8	61.3	4.9	61.6	4.7	59.6
2	4.1	51.5	4.1	51.3	4.0	51.0
3	3.7	46.9	3.6	45.8	3.6	46.1
4	3.2	41.1	3.2	39.9	3.0	37.9
5	2.7	34.1	2.6	33.2	2.5	32.2
6	2.2	27.5	2.1	26.7	2.1	26.4
7	1.7	21.0	1.6	20.1	1.6	19.9
8	1.2	14.6	1.1	13.7	1.1	14.0

## D. Results and discussion

### D.1 Water Surface Deflection

In what follows we will indicate model speeds as the equivalent full scale values in mph. At the maximum speed (60mph), and with the maximum possible water depth, (ie MWC), surface deflection was undetectably small. Figure A4.3 shows the water surface as the train nose passes over a 5mm diameter bolt, fixed to the tank bed as a gauge for the water surface. The deflections, if they exist, are very small, although perhaps the third frame shows a very slight increase in water depth.

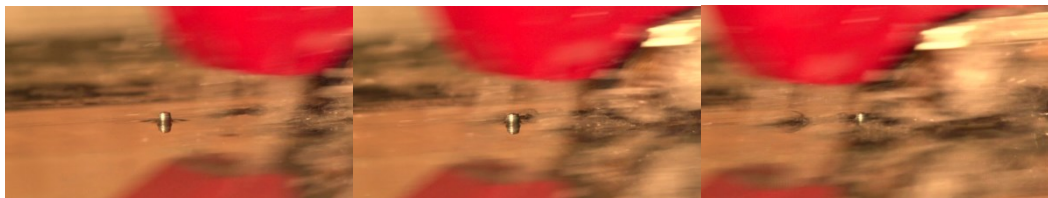


Figure A4.3 Train nose passing over a 5mm diameter bolt at full speed

## D.2 Wheel Splash

### D.2.1 Slight Flange Contact

For starting positions 1 to 5, wheel splash causes wetting of the underside of all bogies (Figures A4.4 to A4.6 at 61mph). Figures A4.4 and A4.5 show that pickup of water by the rear wheels of the front bogie of the locomotive is much greater than that by the front wheels. Splashing onto the front bogie of the locomotive (Figure A4.4 and A4.5) is also noticeably less than that on the rear bogie and the carriage bogies (Figures A4.6 and A4.7). The disturbance to the water surface caused by the front wheels is increasing the amount of contact between the wheel flanges and the water, increasing the pickup with distance along the train as water surface fluctuations increase. Splashing onto the underbody of the locomotive and carriage is limited to the leading portion of the underbody (Figures A4.7 and A4.8).

At 28mph (not shown), splashing onto the Class 43 front bogie is no longer seen, and splashing onto the Class 43 underbody is sporadic. The leading edge of the Mark 3 underbody (being closer to its front bogie) is still continually splashed. At the slowest speed (15 mph), there is still occasional splashing of the three rear bogies and Mark 3 underbody, though this is infrequent.

The bulk of the water picked up by the wheels stays at a low level and has negligible horizontal velocity before falling back to the water surface (Figure A4.9). With regard to the bogies and underbody, the ‘splashing’ is therefore more a process of the train running into the raised water than water being propelled from the wheel against the train. Some of the water (that which remains attached to the wheel until the point where the tangential velocity is near vertically upwards) is propelled upwards into the space between the locomotive and carriage, although this only occurs to a significant degree for the highest speeds. It is also clear from the video that water remains attached to the wheel above the axle.



**Figure A4.4 Splashing on Class 43 locomotive front bogie, SFC, 61 mph**



**Figure A4.5 Splashing from front and rear wheels of the Class 43 locomotive front bogie, SFC, 61 mph**



**Figure A4.6 Splashing on Mark 3 carriage front bogie, SFC, 61 mph**

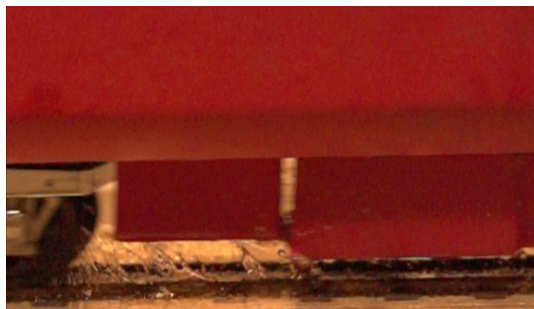


**Figure A4.7 Splashing on Class 43 locomotive underbody, SFC, 61 mph**



**Figure A4.8 Splashing on Mark 3 carriage underbody, SFC, 61 mph**



**Figure A4.9 Splashing between Class 43 locomotive and Mark 3 carriage, SFC, 61 mph**

### D.2.2 Full Flange Contact

With the water level at the top of the railhead, flange contact is increased and water pickup becomes more continuous at high speeds (Figure A4.10 and Figure A4.11) than the SFC, but the water does not appear to be lifted higher. Splashing onto the underbodies does not occur for a noticeably greater length of the underbody, though drain-off from the underbody of the Mark 3 occurs further along the carriage, indicating that there is more water striking it. This is consistent with the more continuous lifting of water into the path of the underbody. Wheel splash onto all bogies and the underbodies of the locomotive and carriage occurs down to a lower speed than in the SFC case (27 mph rather than 33 mph).



**Figure A4.10 Splashing on Class 43 locomotive, FFC, 62 mph**



**Figure A4.11 Splashing between Class 43 locomotive and Mark 3 carriage, FFC, 62 mph**

### D.2.3 Main Wheel Contact

For the SFC and FFC cases, there is little spray to the side of the train. When the main wheel is in contact with the water surface, water must be displaced by the wheel as it passes through, and there is a large increase in the quantity of lateral spray. At the

highest speed (60 mph), this lateral spray is amplified by contact between the lifted water and the sharp, leading edge of the main underbody of the Class 43 (right hand side of Figure A4.12). This effect is not seen for the Mark 3 underbody (Figure A4.13), possibly due to the slope of the leading edge. The second train model was positioned in view of the camera, allowing the amount of water sprayed onto it by the passing train to be (very roughly) seen. This second train was stationary, and was used solely as a backdrop to allow the amount of spray to be estimated. At 60 mph, spray extended up onto the main body of the train (Figure A.4.14), falling only onto the side of the underbody for lower speeds (Figure A4.15) and being negligible for 31 mph and slower (Figure A4.16).

As seen for the difference between SFC and FFC, in terms of splashing of the underbody there is a reduction in the speed required for all bogies to be continuously splashed (20 mph compared to 34 mph and 40 mph for SFC and FFC respectively). The quantity of water lifted by the wheels again increases, but there is no clear increase in the height to which water is lifted while remaining attached to the wheel (Figure A4.17), nor the height to which the water rises once separated from the wheel. This may be due to the wheels having the same rotational speed in each case.



**Figure A4.12 Splashing from the Class 43 locomotive, MWC, 60 mph**



**Figure A4.13 Splashing from the Mark 3 carriage, MWC, 60 mph**



**Figure A4.14 Spray onto a parallel, stationary train, MWC, 60 mph**



**Figure A4.15 Spray onto a parallel, stationary train, MWC, 38 mph**

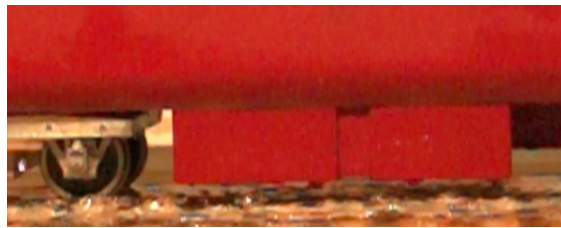


**Figure A4.16 Spray onto a parallel, stationary train, MWC, 32 mph**

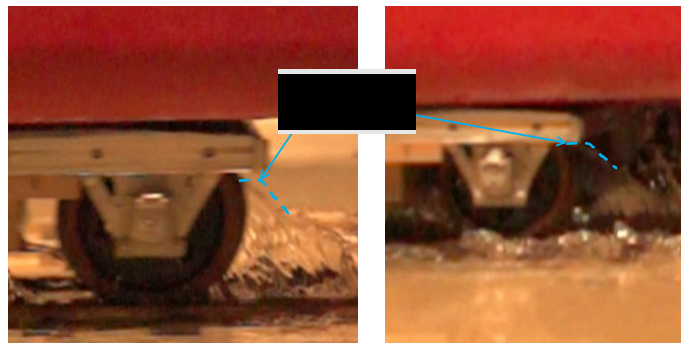


**Figure A4.17 Water attachment to the wheel, (left) SFC, 34 mph and (right) MWC, 32 mph**

## E. Speed Measurements for Wheel Drag Validation

Single runs from each starting point were made for two water depths, 2mm and 6mm above the railhead (the former approximately equal to MWC above). A decrease in speed is seen with increased water depth. This magnitude of this reduces in absolute terms as the run speed reduces (Table A4.2 and Figure A4.18).

**Table A4.2 Train model speeds and full-scale equivalent speeds for over railhead flood water**

Starting Position	2mm Over Railhead		6mm Over Railhead	
	V (model, m/s)	V (full, mph)	V (model, m/s)	V (full, mph)
1	4.8	60.09	4.9	57.2
2	4.1	51.11	4.1	48.2
3	3.7	45.62	3.6	43.3
4	3.2	39.23	3.2	37.4
5	2.7	32.96	2.6	31.1
6	2.2	26.93	2.1	25.7
7	1.7	20.58	1.6	19.2
8	1.2	14.15	1.1	13.0

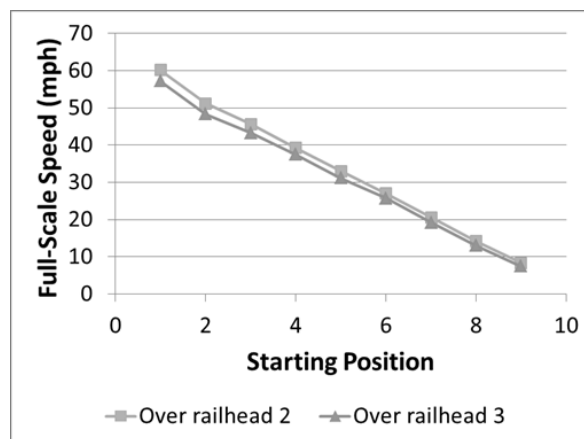


**Figure A4.18 Train speed at different over railhead water depths by starting position**

Using the sets of ten runs made at the same starting position and with the same water depth, the run-to-run variation is seen to be negligible in comparison to the variation with water depth (Figure A4.19). Mean values of each set of runs is given in Table A4.3.

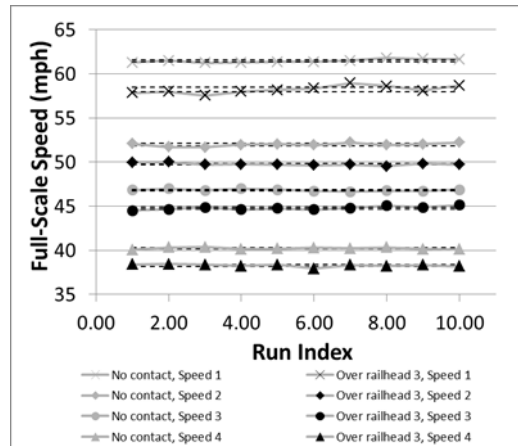


**Figure A4.19 A comparison of train speeds seen in multiple runs using the same starting position and water depth configuration. Dotted lines indicate the 95% confidence interval around the sample mean.**

**Table A4.3 Train model speeds and full-scale equivalent speeds for over railhead flood water**

	No Contact		6mm Over Railhead	
	m/s (model-scale)	mph (full-scale)	m/s (model-scale)	mph (full-scale)
Speed 1	4.86	61.46	4.60	58.22
Speed 2	4.11	51.97	3.93	49.75
Speed 3	3.70	46.81	3.54	44.78

## Appendix 5 Validation and use of the free surface model

## A. Determination of parameters and solutions of the equations

It was noted in Appendix 2 that the equations as derived imply that the water surface height variations caused by aerodynamic effects will be small in comparison to those caused by wheel effects. This section will thus explore the relationship between the effects.

We assume a 200m long train of eight coaches, with 5m length of bogies at the ends of each of the eight vehicles, moving at a speed of 20 mph. We assume the water depth is at rail height. From the CFD results of Appendix 3a, the peak pressure coefficient characteristics around the train nose are as follows

- Passenger train peak to peak values: 0.70
- Passenger train peak to peak distance: 4 m
- Freight train peak to peak values: 1.5
- Freight train peak to peak distance: 2 m

These coefficient values can be compared with the experimentally measured values for the Eurostar Class 373 reported in [A5.1] of 0.65, which suggests they are of the correct order. The freight train nose pressures are thus the more severe, and we will use them in what follows. We model the pressure transient using the coefficient form:

$$C_p = A_1 x e^{-A_2 |x|} \quad (A5.1)$$

Values of the scaling factors  $A_1$  and  $A_2$  of 1.0 and 0.5 result in pressure coefficient curves of the correct size and spread to represent the freight train. Similarly Appendix 2 shows that the friction coefficients around passenger and freight trains are approximately given by

- Passenger train - approximately 0.001
- Freight train peak – approximately 0.002

Again these figures can be compared with those in the published literature. All previous authors measured the friction over an unflooded track and thus the measured values represent the roughness over ballast / slab track and sleepers. The results of [A5.2] give values for high speed trains over slab and ballasted track of the order of 0.001, whilst the results of [A5.3], [A5.4] and [A5.5] all give somewhat higher values of around 0.006 to 0.010 for slab track and sleepers, and 0.03 to 0.05 for ballasted track and sleepers. The results of Appendix 3a for smooth water surfaces thus seem to be consistent with earlier work. In what follows we again assume the values for the freight train case as being the most arduous.

The physical model tests did however allow the wheel / spray component of the model to be verified. Firstly, the data for model speeds passing through different water depths allowed the value of the drag coefficient  $C_D$  to be determined. It is straightforward to show that the drag coefficient is given by

$$C_D = \frac{2M}{A_w \rho_w X} \frac{\Delta v}{v} \quad (\text{A5.2})$$

where  $M$  is the mass model (=6.65kg),  $A_w$  is the area of the wheel in contact with the water,  $\rho_w$  is the density of water (=1000kg/m<sup>3</sup>),  $X$  is the distance the model travels through the water (3.18m) and  $\frac{\Delta v}{v}$  is the fractional loss of model speed from the no-water contact case. Appendix 4 reports on a series of experiments where repeated measurements were made of the velocities of the train model with no water contact and with the water 6mm above the rail top (19cm full scale). The values for  $\frac{\Delta v}{v}$  and drag coefficient calculated from these experiments are given in table A5.1 below. There is some suggestion of an increase in drag coefficient as the speed increases, although this is far from conclusive. This was not unexpected for two reasons – the decrease in the effects of surface tension as the speeds increase, and the increased energy loss due to spray formation. The question thus arises as to how this drag coefficient variation should be parameterised. Whilst the physical model tests are useful in identifying trends, it can be expected that the results contain significant scale effects and should be viewed with some circumspection. However, as there is no other data available at present, we use the values presented above to derive the following drag coefficient characteristic. We simply assume the following characteristic based on these results and an estimation of the Froude number at which surface tension effects inhibit water motion

$$\begin{aligned} C_D &= 0 && \text{for } F < 2 \\ C_D &= 0.122(F - 2) && \text{for } 2 < F < 13.5 \\ C_D &= 1.4 && \text{for } F > 13.5 \end{aligned} \quad (\text{A5.3})$$

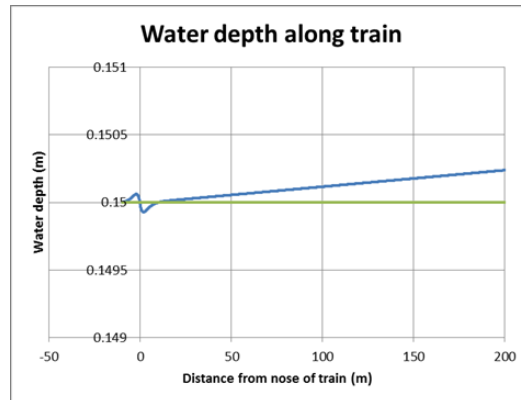
This equation is wholly empirical and should only be regarded as provisional, and more work is required in this area.

**Table A5.1 Calculation of drag coefficient**

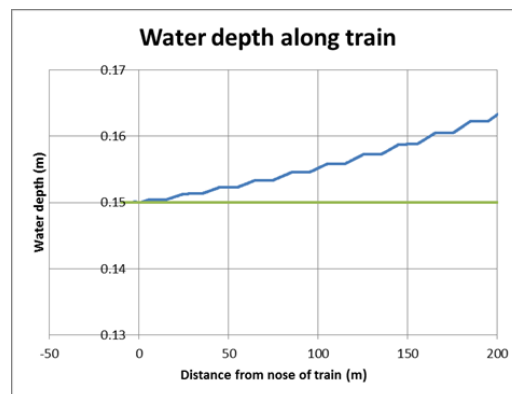
$v$	$\frac{\Delta v}{v}$	$F$	$C_D$
4.86	0.0526	14.7	1.40
4.11	0.0428	12.5	1.14
3.70	0.0432	11.2	1.15

Figure A5.1 shows the water surface displacement just considering the aerodynamic effects, and Figure A5.2 shows the water surface displacement due to just the wheel effects. It is immediately clear that the wheel effects are very much greater than the aerodynamic effects – an observation which is generally true for all reasonable values of the friction and pressure parameters. Thus the hypothesis that one of the mechanisms

of water uplift is due to aerodynamic forces must be discounted, and thus wheel drag effects are the dominant cause of water uplift. Thus equation (A2.21) can be used in the calculation of water depths.



**Figure A5.1 Calculated water depths along train – aerodynamic effects only**



**Figure A5.2 Calculated water depths along train –wheel effects only**

## B. Verification of model

The free surface model can be verified on a number of levels. The first is whether or not it produces the overall observed flow patterns. The YouTube video of a Class 43 passing through flood water [A5.6] is instructive in this regard – see the screenshots at Figure A5.3. The train speed is around 80 mph in this case. It shows that there is little disturbance to the water surface ahead of the train, but the amount of spray from the wheels increases along the length of the train. This is consistent with the results presented above, and the effect of the train wheelsets cause the water surface to rise underneath the train, and thus there will be greater contact between the wheels and the water causing more spray.



**Figure A5.3 Class 43 passing through flood water at Draycott [A5.6]**

At much lower train speeds there is little effect of spray as would be expected. Figure A5.4 shows a Class 220 passing at around 5 mph across a flooded crossing, and a steady bow wave can be seen ahead of the wheelsets [A5.7].



**Figure A5.4 Class 220 passing through a flooded crossing [A5.7]**

Finally, at the other end of the scale, the screen shots from [A5.8] show a blunt nosed train in Buenos Aires passing at around 30 mph with a huge bow wave of spray ahead of it – possibly caused by water spray from the front bogie being projected forwards at these speeds (Figure A5.5)



**Figure A5.5 Train passing through flood water in Buenos Aires [A5.8]**

This Appendix, however, clearly predicts that there is a deformation of the water surface ahead of the train caused by the nose pressure transient. It was hoped at the start of the project that this would be verified by the physical model tests and the unsteady CFD calculations. Unfortunately it became clear that both of these techniques, which were carried out at model scale, were badly influenced by surface tension effects, which damped out any free surface variation. Reference [A5.9] shows that for capillary waves the wavelength at which inertial effects are equal to surface tension effects is of the order of 2 cm, with surface tension effects dominating for lower wavelengths. The length scale of the surface deformations in the physical model tests and in the model scale CFD tests were of that order. In the physical model tests reported in Appendix 4, it was not possible to see any significant free surface variation at all. However in the model scale unsteady CFD tests reported in Appendix 3b surface deformations can be seen. Although these are small as would be expected, nonetheless they are of the correct form – with an increase in water surface height, followed by a decrease around the nose, and then an increase along the length of the train. Further unsteady CFD calculations were carried out for full scale parameter values but it did not prove possible to obtain convergence of these results. Nonetheless, the model is broadly consistent with the surface profiles observed at full scale and in the unsteady CFD calculations.

Secondly the physical model tests showed that wheel spray increased markedly when there is full wheel contact with the water i.e. when the water is above the railhead, and when the vehicle speed is above a value of around 20 mph at full scale. For flange only contact, then the speed at which there is significant spray is somewhat higher at around 30 mph. Whilst one must be circumspect in the interpretation of these results as modelling effects can be expected to be significant, they do suggest that where there is flange contact of the water and the speed is greater than 30 mph, or where there is full wheel contact and the speed is greater than 20 mph, the effects of spray might be significant.

## C. Model results

As the model results depend only on the wheels, there is no need to carry out calculations for different train types. In this section, we present calculations for the bogie arrangement outlined above in Section A for three different water depths – around the mid-height of the flange (1.5cm below the top of the rail), top of rail, and 5cm above the top of the rail, for speeds of 5, 10, 20, 30 and 50 mph. These results are shown in Figures A5.6 to A5.8 below. The stepwise nature of the data is apparent, due to water lift behind individual bogies. For water below rail height, but in contact with the flanges (Figure A5.6) there is only a small water depth increase along the train, although as noted above, for 30 mph and above one might expect significant spray. When the water is at the railhead (Figure A5.7), there is a more significant increase in water depth particularly at the higher speeds. For a water depth of 5cm above the top of the railhead, water depth increases (and the associated spray) become significant for speeds of 20 mph and above.

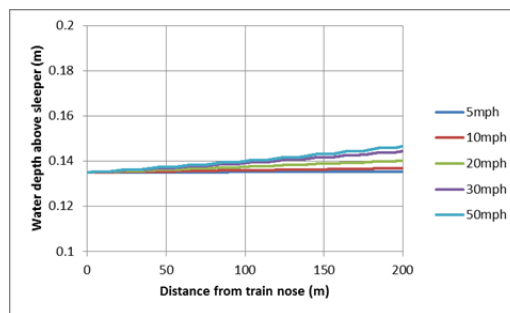


Figure A5.6 Water surface depths – water below rail head, in contact with flange

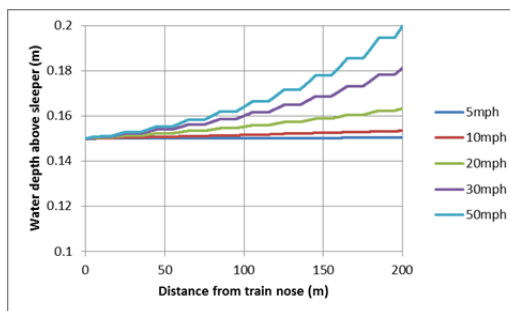
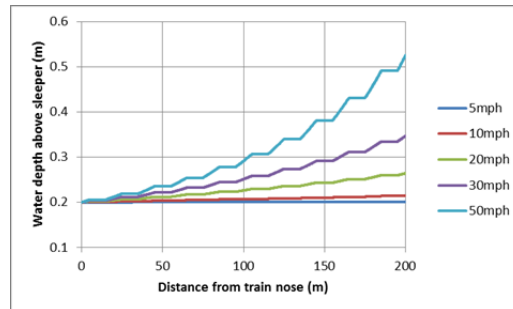


Figure A5.6 Water surface depths – water at top of rail head



**Figure A5.6 Water surface depths – water below rail head, in contact with flange above top of rail head**

## D. References

- A5.1 Quinn A.D., Hayward M., Baker C. J., Schmid F., Priest J., Powrie W. (2010) “A full-scale experimental and modelling study of ballast flight under high speed trains”, *Journal of Rail and Rapid Transit* 224, 61- 74
- A5.2 Saat M.R., Bedini-Jacobini F., Tutumluer E., Barkan C. (2015) “Identification of High-Speed Rail Ballast Flight Risk Factors and Risk Mitigation Strategies – Final Report”. FRA Report DOT/FRA/ORD-15/03
- A5.3 Deeg P., Jonsson M., Kaltenbach H-J., Schober M., Weise M. (2008) “Determination of train induced aerodynamic loads on the trackbed”, *Bluff Body Aerodynamics and its Applications*, Milan
- A5.4 Kaltenbach H-J., Gautier. P-E, Agirre G., Orellano A., Schroeder-Bodenstein K., M. Testa M., Th. Tielkes Th. (2008) “Assessment of the aerodynamic loads on the trackbed causing ballast projection: results from the DEUFRAKO project Aerodynamics in Open Air (AOA)”, *World Congress on Rail Research S.2.3.4.1*
- A5.5 Lazaro B., Gonzalez E., Rodriguez M., Osma S., Iglesias J. (2008) “Characterization and Modeling of Flying Ballast Phenomena in High-speed Train Lines”, *World Congress on Rail Research*, Seoul, South Korea
- A5.6 YouTube (2015a) <https://www.youtube.com/watch?v=oddL3Jpn6UI>
- A5.7 YouTube (2015b) <https://www.youtube.com/watch?v=iQRT2jZxeOg>
- A5.8 YouTube (2015c) <https://www.youtube.com/watch?v=UUJ43L35E7c>
- A5.9 Lighthill, M.J. (1978), *Waves in fluids*, Cambridge University Press, 504 pp., ISBN 0-521-29233-6, OCLC 2966533

RSSB R&D Programme  
Floor 4, The Helicon  
1 South Street  
London  
EC2M 2RB

[enquirydesk@rssb.co.uk](mailto:enquirydesk@rssb.co.uk)

[http://www.rssb.co.uk/research-development-innovation/  
research-and-development](http://www.rssb.co.uk/research-development-innovation/research-and-development)